The transcription factor CLAMP is required for neurogenesis in *Drosophila melanogaster*.

Maria A. Tsiarli [1,2,6*], James A. Kentro[1,5,6], Ashley M. Conard [1,3,4], Lucy Xu [1], Erica Nguyen[1], Kate O'Connor-Giles[5,6], Erica N. Larschan [1,6*]

[1] Department of Molecular Biology, Cellular Biology and Biochemistry, Brown University, Providence, RI 02912, USA

[2] Department of Neurobiology, Harvard Medical School, Boston, MA Department 02115, USA

[3] Center for Computational and Molecular Biology, Brown University, Providence, RI, 02912;

[4] Computer Science Department, Brown University, Providence, RI, 02912

[5] Department of Neuroscience, Brown University, Providence, RI, USA

[6] Carney Institute for Brain Science, Brown University, Providence, RI, USA

* corresponding author

Contact information

Maria A. Tsiarli: maria_tsiarli@brown.edu; maria_tsiarli@hms.harvard.edu

Ashley M. Conard: ashley_conard@brown.edu

Lucy Xu: lucy_xu@alumni.brown.edu

Erica Nguyen: erica_nguyen@alumni.brown.edu

Erica N. Larschan: erica_larschan@brown.edu

Abstract

Neural stem cell (NSC) differentiation is controlled by cell-intrinsic and external signals from the stem cell niche including niche surface glia (SG). However, the mechanisms by which transcription factors drive NSC differentiation within the niche remain largely unknown. Here, we show that the *Drosophila* melanogaster transcription factor, Chromatin-linked adaptor for MSL proteins (CLAMP) is required for regulation of stemness and proliferation of NSCs, especially of the optic lobe (OL). CLAMP promotes transcription of genes involved in stemness, proliferation, and glial development and represses transcription of genes involved in neurogenesis and niche survival. Consistent with transcriptional changes, CLAMP promotes NSC proliferation and niche SG production, while lack of CLAMP severely and specifically impacts OL development. To identify potential mechanisms by which CLAMP may regulate brain development, we examined CLAMP motifs and available CLAMP ChIP-seq data to determine which genes may be direct versus indirect targets. CLAMP motifs are present at many target genes including the glial-determining gene, *glial cells missing,* while *Tailless,* the master regulator of OL- development is directly bound by CLAMP. In accordance to these results, in larval OL NSCs lacking CLAMP, Tailless levels are decreased dramatically, suggesting that CLAMP controls OL neurogenesis *via* Tailless. Overall, our results suggest that CLAMP regulates a transcriptional program which drives NSC proliferation and differentiation *via* cell-intrinsic and niche-dependent mechanisms that involve transcriptional regulation of *Tailless* and niche glia.

53 **Introduction**

54

55 Brain development is an extremely complex yet carefully orchestrated process, regulated along
56 spatiotemporal axes. For the formation of the functional brain circuitry to take place, neural stem cells
57 (NSCs) must undergo multiple rounds of divisions and lineage decisions at each step of the process are
58 governed by specific transcription factors (TFs) (KONSTANTINIDES *et al.* 2018). In addition to the intrinsic
59 developmental program, external metabolic and paracrine signals constitute another layer of developmental
60 control over NSCs. Specifically, NSCs are part of a specialized microenvironment, the stem cell niche
61 (SCADDEN 2006), which plays an architectural and nurturing role for the NSCs and their progeny.
62 Moreover, the niche serves as a hub for the relay of metabolic and developmental signals that regulate
63 differentiation of NSCs in order for the proper sequence of developmental events to be maintained (SPEDER
64 AND BRAND 2018). In mammals, the stem cell niche is composed of various cell populations including
65 neurons, glial cells, resident immune cells, the microglia, blood vessels which along with endothelial cells
66 and glial cells form the blood-brain-barrier (DANI *et al.* 2019). In *Drosophila*, the stem cell niche consists
67 of NSCs, NSC progeny and glial cells of various types that are vital to the maintenance of the homeostatic
68 balance required for proper neurogenesis to take place (HINDLE AND BAINTON 2014; SPÉDER AND BRAND
69 2014; BAILEY *et al.* 2015; KANAI *et al.* 2018; SPEDER AND BRAND 2018; RAMON-CAÑELLAS *et al.* 2019;
70 YUAN *et al.* 2020). However, little is understood about the gene regulatory mechanisms that generate the
71 stem cell niche.

72

73 In *Drosophila melanogaster* neurogenesis occurs at two distinct stages: the embryonic and post-embryonic
74 stages (HARTENSTEIN AND CAMPOS-ORTEGA 1984; PROKOP AND TECHNAU 1991). The *Drosophila* central
75 nervous system (CNS) is composed of the central brain (CB), the optic lobe (OL) and the ventral nerve cord
76 (VNC). During the embryonic stage, CB neural stem cells (neuroblasts in *Drosophila*) proliferate to
77 generate primary neurons until they become quiescent at the end of the embryonic stage. The optic lobe

primordium which would form the OL, is generated by epithelial cells of the posterior procephalic region between embryonic stages 11-13 (RAMON-CAÑELLAS *et al.* 2018). Between stages 12 and 13, the OL primordium invaginates and attaches at the ventrolateral surface of the brain and embryonic OL neuroblasts (EONs) are formed (HAKES *et al.* 2018). EONs proliferate briefly to generate glial and neuronal progeny and also enter quiescence (HAKES *et al.* 2018; CONTRERAS *et al.* 2019b). During the early larval stage, concurrent with the initiation of larval feeding, metabolic signals impinge on the NSCs and cause exit from quiescence and initiation of neurogenesis.

Neural stem cells divide asymmetrically, such that in each division they generate a new NSC and a daughter cell which will generate glial and/or neuronal progeny (EGGER *et al.* 2008). For the appropriate asymmetric division to take place, polarity determinants have to be sequestered on the apical and basal sides of the mother NSC: the apical complexes are inherited by the new NSC and maintain the proliferating state, whereas basal proteins are inherited by the daughter cell and will direct it to generate differentiated lineages. The Par protein complex which is apically localized also directs the localization of the basal determinants. Moreover, Par complex proteins such as the *Inscuteable* (Insc) and *Partner of Inscuteable (Pins)* regulate the orientation of the mitotic spindle which determines how the cleavage furrow will form during the division of the NSC (GALLAUD *et al.* 2017; CREWS 2019). Additionally, in the optic lobe, sequential expression of transcription factors in proliferating NSCs, including of *Tailless* and *Notch*, regulates the temporal generation of diverse progeny types (LI *et al.* 2013; BERTET *et al.* 2014).

In the *Drosophila,* five distinct CNS glial types are identified based on morphological, positioning and molecular profile criteria: perineurial (PG), subperineurial glia (SPG), cortex glia (CG), astrocyte-like and ensheathing glia (YILDIRIM *et al.* 2019). Perineural glia ~~are found on the outside layer of the CNS and~~ serve a nurturing role for the development and function of the NSCs and also regulate NSC proliferation (KANAI *et al.* 2018). Reciprocally, the proliferating NSCs regulate their proliferation and the survival of PG *via* a mechanism that implicates secretion the Glass bottom boat protein~~.~~ With the initiation of larval feeding,

104 SPG and PG contribute to the reactivation of quiescent NSCs (SOUSA-NUNES *et al.* 2011; SPÉDER AND
105 BRAND 2014; KANAI *et al.* 2018) *via* fat body signaling and induction of insulin secretion from SPG. In
106 conditions of oxidative stress and hypoxia, SPG and CG form lipid droplets (LDs) which protect NSCs
107 from oxidative stress (BAILEY *et al.* 2015; KIS *et al.* 2015). CG forms a bespoke membrane chamber around
108 dividing NSCs and their progeny, thus providing protection to the proliferating NSCs and their niche, and
109 serving as individual spatial units for each expanding NSC and its progeny (SPEDER AND BRAND 2018). A
110 special subtype of CG, *mir8*$^{+}$ surface-associated CG, controls neurogenesis in the OL (MORANTE *et al.*
111 2013; RAMON-CAÑELLAS *et al.* 2018; YILDIRIM *et al.* 2019). Thus, niche glia are important for the function
112 of NSCs. However, the molecular mechanisms that direct the functional and nurturing relationship between
113 niche glia and NSCs remain poorly understood.
114
115 Here we define a role for the essential CLAMP zinc finger TF (SORUCO *et al.* 2013b) in neurogenesis which
116 is partly mediated by transcriptional regulation of key TFs controlling stemness and proliferation, and partly
117 *via* niche glia. CLAMP was discovered as part of a screen for factors that are necessary for the function of
118 the dosage compensation machinery in *Drosophila melanogaster* males (LARSCHAN *et al.* 2012). CLAMP
119 is essential for viability of both males and females and has transcriptional targets on all chromosomes, with
120 a stronger binding affinity on the X chromosome (SORUCO *et al.* 2013b; URBAN 2017). Since its first
121 characterization as a required link for the MSL complex to bind to the X-chromosome (SORUCO *et al.*
122 2013a; TIKHONOVA *et al.* 2019), CLAMP is emerging as a multifaceted transcription factor with multiple
123 roles including chromatin organization (KAYE *et al.* 2017), histone locus function (RIEDER *et al.* 2017) and
124 regulation of Pol II (URBAN *et al.* 2017). The identification of *Clamp* (CG1832), as a functional interactor
125 of *embryonic lethal abnormal visual system* (*elav*) and *erect wings* (*ewg),* critical regulators of embryonic
126 and post-embryonic neural development, suggested a potential neuronal role of CLAMP (HAUSSMANN *et*
127 *al.* 2008; HAUSSMANN AND SOLLER 2010b). Therefore, we hypothesized that CLAMP is a TF which
128 regulates neuronal development and NSC biology.
129

130 To test our hypothesis, we investigated the role of CLAMP in nervous system development. We found that
131 CLAMP is important both for neuronal and glial cell generation and regulates NSC proliferation *via* cell-
132 intrinsic and niche-dependent mechanisms. We used a CRISPR/Cas9-generated frameshift mutant in the
133 *clamp* gene which eliminates the expression of the CLAMP protein (URBAN 2017). Using this approach,
134 we observed that lack of CLAMP results in brain development defects. Specifically, *clamp* null mutants
135 have a smaller brain than controls, with the most prominent defect observed in the optic lobe which is
136 almost entirely lost. To determine the transcriptional networks affected by the absence of CLAMP, we
137 performed mRNA-sequencing data of *clamp* mutant embryos and larval brains, followed by gene ontology
138 (GO) analysis, which revealled that CLAMP positively regulates stemness/NSC proliferation genes and
139 glial-development genes.
140
141 To specifically determine which of the differentially expressed genes (DEGs) are under direct CLAMP
142 regulation, we performed binding motif analysis which revealed that CLAMP motifs are present at key
143 neurogenesis genes such as *bazooka, gbb* and the glial-development regulator, *glial cells missing.* To further
144 validate direct regulation of the identified DEGs by CLAMP, we proceeded with mining available CLAMP
145 embryo ChIP-seq data. Importantly, this analysis revealed that *Tailless,* the master regulator of OL
146 development, is both regulated and bound by CLAMP, suggesting that it is a direct target and can underlie
147 the profound defects in OL development seen in *clamp* null mutants.
148
149 To further explore the relation between CLAMP and Tailless, we proceeded with immunostaining in *clamp*
150 null mutant brains using NSC and glia markers and Tailless. This revealed that *clamp* null mutants exhibit
151 a brain-wide reduction in proliferating NSCs and surface glia and a profound defect in the development of
152 the OL, similar to the phenotype seen in *Tailless* knock-down brains (GUILLERMIN *et al.* 2015).
153 Furthermore, knock-down of *clamp* in glia but not in neurons, revealed that NSC proliferation and glia
154 generation are partly regulated *via* glial CLAMP.
155

Our results support a model in which CLAMP regulates a transcriptional program which drives NSC proliferation and differentiation *via* cell-intrinsic and niche-dependent mechanisms that involve direct transcriptional regulation of *Tailless* and niche glia.

181 ***Materials and Methods***

182

183 ***Fly Strains***

184

185 Fly stocks used in this study were as follows: y^1w^1 wild type controls, *clamp*^{2} null, and *CLAMP* rescue lines,
186 which were generated by Urban et al.(2017) and described therein *(URBAN 2017)*. Briefly, the *clamp* null,
187 is a CRISPR-Cas9 generated frameshift mutation which abolishes CLAMP protein expression, whereas the
188 *clamp* rescue was generated by introduction of a full CLAMP rescue construct on chromosome 3L. For the
189 RNAi experiments the following lines were used: *repo-GAL4*, *elav*^{c155} (*elav-GAL4*) and UAS-*clamp-RNAi,*
190 all obtained from the Bloomington Stock Center. All crosses were done at 25ºC and a 12-hour light/dark
191 cycle.

192

193 ***Immunostaining***

194

195 The following antibodies were used: Rabbit anti-CLAMP (1:200, Abcam custom made), mouse anti-Repo
196 (1:50, Developmental Studies Hybridoma Bank (DSHB) 8D12), rabbit anti-DCP1 (1:100, Cell Signaling),
197 rat anti-Deadpan (Dpn, 1:100, Abcam), rat anti-Elav (1:50, DSHB), mouse anti-Prospero (Pros, 1:30,
198 DSHB), PCNA (PC10, Abcam), Nc82 (1:10, DSHB), rabbit anti-Tailless (Kindly provided by Dr James
199 Sharpe, EMBL-Barcelona). Secondary antibodies used were Alexa Fluor Conjugated A405, A488, A568,
200 A647 (1:1000, Invitrogen). A standard staining protocol was used.

201

202 ***Quantification of marker-positive and superficial glia cells***

203

204 To quantify superficial glia, 3-µm projections (z-projections of three 1-µm optical sections) of the dorsal
205 surface of third instar larval brain hemispheres stained for Repo were used and quantified manually using
206 Adobe Photoshop, as exemplified by Kanai et al. (2018). Six hemispheres were quantified for each

genotype. The same approach was used to quantify marker positive cells i.e., Dpn, Pros and EdU. To ensure consistency between samples of control and the *clamp* mutant brains basic morphological features based on DAPI staining in combination with stack depth were monitored.

Image acquisition and processing

Fluorescent images were acquired using an inverted Olympus FLUOVIEW FV1000 confocal laser scanning microscope or a Leica TCS SP2 AOBS DMIRE2 inverted scanning confocal microscope. Adobe Photoshop was used to adjust brightness and contrast in images and ImageJ (or Fiji (Schindelin et al., 2012)) was used to analyzed images, while Adobe Illustrator was used to compile figures.

EdU Incorporation

EdU incorporation in proliferative brain cells, was performed using Click-It Edu Alexa Fluor A488 (Thermo Fisher Scientific, MA, USA) in an adaptation of Tastan and Liu (2015) (TASTAN AND LIU 2015) method. Briefly, samples were dissected in ice-cold Graces media and then transferred in Graces media containing 5μg/ml of EdU, for 2 hours at room temperature. Then, samples were washed in 0.1% PBST and fixed in 4% PFA in 0.1% PBST, for 20 min at room temperature. Next, tissues were washed in 5% HINGS in 0.1 % PBST and then permealized in 0.5% PBST for 20 min (RT). After this step, the EdU Click It steps were followed according to the manufacturer's instructions and then additional antibody staining was followed as described above.

Larval Staging

Third Instar larvae crawling on the vial walls were selected to be mid/late stage using the bromophenol blue method adjusted from Maroni and Stamey (1983) (MARONI AND STAMEY 1983), using 0.05% w/v

233 bromophenol blue-containing fly food. To control for variations in brain size due to crowding, experiments
234 were done under controlled density conditions. Specifically, a set number of mated males and females were
235 allowed to mate for 5 hours and then removed from the vial. Additionally, the progeny number was
236 evaluated to validate that we did not have large deviations between control and *clamp* mutant larvae
237 numbers.
238
239 ***RNA extraction and RNA sequencing***
240
241 Mid/late third instar larvae were staged using the bromophenol blue method and larval brains were dissected
242 in ice-cold PBS, collected in TRIzol until RNA extraction was performed using the phenol-chloroform
243 method. Each biological replicate was generated by pooling at least 12 larval brains. mRNA-focused
244 sequencing libraries were constructed from total RNA using the Illumina Truseq RNA Library kit v2
245 according to the manufacturer's instructions (no strand-information). Paired-end 100 bp or 50 bp was
246 performed on an Illumina HiSeq2500 sequencer in High-Output mode at the MGH NextGen Sequencing
247 Core. Four biological samples were used per experimental condition. As the control group, we used the
248 CLAMP rescue line in which the wild type CLAMP gene was inserted into an attP site under the control of
249 its endogenous promoter (URBAN 2017).
250
251 ***RNA sequencing data analysis and Differential Gene Expression Analysis***
252
253 RNA-seq reads were processed using FastQC (ANDREWS 2010) with default parameters to check the
254 quality of raw sequence data and filter out sequences flagged for poor quality, and aligned using HISAT2
255 (KIM *et al.* 2015). Then read counts per gene were generated via HTSeq (ANDERS *et al.* 2015) using the
256 *Drosophila melanogaster* genome dm6 (BDGP6) genome as reference. Differential gene expression
257 analysis was performed using DESeq2 (LOVE *et al.* 2014). *gProfiler* was used for GO analysis (RAUDVERE
258 *et al.* 2019). Using TIMEOR (CONARD *et al.* 2020) the temporally differentially expressed genes where

259 displayed in interactive expression cluster-maps along the developmental time scale (see Supplementary
260 files: *Embryo_heatmap* and *L3_brain_heatmap*), from which additional, GO analysis was performed by
261 TIMEOR *via* clusterProfiler (YU *et al.* 2012) to evaluate for possible gene networks.
262
263 ***Clamp Binding motifs***
264
265 We used FIMO (GRANT *et al.* 2011) to identify individual CLAMP motif occurrences within ± 1KB from
266 the transcription start and end sites for all genes within each gene trajectory cluster. The position weight
267 matrix used (KAYE *et al.* 2018) highlights the CLAMP motif independently of GAF binding potential. The
268 specific command used is: *(fimo --oc $OUTPUT_DIR/ CLAMP_PWM.txt $geneList)*
269
270 ***Average profiles***
271
272 The average control-normalized read depth across a set of regions was plotted using deepTools
273 computeMatrix and plotProfile. The read depth source are ChIP-seq data in the ENCODE database for
274 CG1832 (Clamp) from mixed sex embryos (0-24hrs), part of the modERN project
275 (https://www.encodeproject.org/experiments/ENCSR858HYS/). The regions were chosen as each set of
276 differentially expressed genes (DEGs) from the *clamp* null versus *clamp* rescue RNA-seq experiments in
277 embryo and third instar larvae. These were kept as all DEGs in an experiment and as separate images for
278 up or down regulated genes in the absence of *clamp*. The gene regions were scaled to match positions of
279 the transcription start sites (TSS) and transcription end sites (TES) with 3K base pairs shown on either side
280 of the gene.
281
282 ***Western Blotting***
283

284 Larval brains were dissected from wandering third instar larvae in ice-cold 0.7% saline and transferred in
285 PBS + 0.3% Triton X-100 on ice. Liquid was carefully removed, then samples were frozen in liquid
286 nitrogen and stored at -80°C until use. Approximately ten brains were collected per biological replicate.
287 For protein extraction, 50 µL of ice-cold RIPA buffer (150 µL1M Tris-HCl pH 8, 12 µL 0.5M EDTA, 0.003
288 g sodium deoxycholate, 15 µL 20% SDS, 90 µL 5M NaCl, 30 µL 50x protease inhibitor, and 2700 µL
289 water) was added to each sample. Samples were homogenized using an electric handheld homogenizer and
290 disposable plastic pestle. After homogenization, the pestle was rinsed with an additional 50 µL of RIPA for
291 a total volume of 100 µL per tube. Samples were rotated at 4°C for 1-2 hours. Protein concentration was
292 quantified using the Qubit Protein Assay kit (Thermo Fisher Scientific).
293
294 ***Statistical Analysis***
295
296 Excel and GraphPad Prism were used for statistical analysis. Bar graphs were generated using the mean
297 and standard error of the mean (SEM) for each sample. Statistical significance was determined using an
298 unpaired Student's t-test.
299
300 ***Data Availability Statement & Correspondence***
301
302 Data and materials generated in this study are available upon request from the corresponding authors.
303 Transcriptomic data have been deposited in Gene Expression Omnibus (GEO) Database, under the
304 accession number GSE148704.
305
306
307
308
309

310 **Results**

311

312 ***CLAMP is expressed throughout the larval nervous system and in proliferating neuroblasts.***

313

314 CLAMP is maternally deposited at both the protein and RNA levels and therefore *clamp* transcript and
315 CLAMP protein levels are present at high levels during embryogenesis (RIEDER *et al.* 2017). Near the end
316 of embryogenesis (16-18 hours), during tissue differentiation and the cessation of the first wave of
317 neurogenesis, *clamp* transcript levels show a reduction followed by a sharp increase between 20-24 hours
318 and then a decrease throughout the post-embryonic neurogenesis period (Fig. 1a). Tissue-specific
319 expression data from the modENCODE Development RNA-Seq Collection (GRAVELEY *et al.* 2011;
320 BROWN *et al.* 2014)/Flybase (THURMOND *et al.* 2019) show that *clamp* is highly expressed in the third (L3)
321 central nervous system (Fig.1b).

322

323 To define the role of CLAMP in neural development, we mapped its expression in the developing L3 central
324 nervous system using immunofluorescence. We found that CLAMP is ubiquitously expressed in the nucleus
325 throughout the larval nervous system, both in cells of the brain and the VNC (Figs.1c and d). Interestingly,
326 a subset of neuronal processes in the VNC also show protein localization of CLAMP, suggesting that it
327 may be transported to neuronal arborizations (Fig. 1c, axonal processes indicated by arrows). Co-staining
328 of proliferating cell nuclear antigen (PCNA) which labels proliferating cells, revealed that CLAMP is
329 expressed in proliferating NSCs (Figs.1e-h), both in the central brain and the OL (Figs.1f-h, cyan and yellow
330 arrows, respectively). CLAMP colocalizes with PCNA both in CB neuroblasts and ganglion mother cells,
331 as identified based on their size difference (Figs.1f-h, cyan and magenta arrows, respectively).

332

333 ***Loss of CLAMP disrupts larval development***

334

335 To determine the role of CLAMP in nervous system development, we characterized brain development in
336 *clamp*^{2} null mutants that we previously generated in our lab using CRISPR (URBAN 2017). In these mutants,
337 a frameshift mutation in the *clamp* gene abolishes expression of CLAMP protein (URBAN 2017) (from here
338 on referred to as *clamp* null). Due to CLAMP's early role in the recruitment of the dosage compensation
339 complex in males (SORUCO *et al.* 2013b), the majority of male larvae die at the L2 stage. In contrast, female
340 larvae die at the late L3/prepupa stage (URBAN 2017). Because of our interest in the essential role of
341 CLAMP independent of dosage compensation and due to the small number of male *clamp* null larvae, we
342 focused on female L3 larvae. Comparison of *clamp* null L3 larvae to stage-matched controls (see Materials
343 and Methods) revealed that *clamp* larvae are significantly smaller than controls (Figs.2a and b).
344 Furthermore, macroscopic examination of the central nervous system (CNS) of *clamp* null larvae revealed
345 that their brains are also significantly smaller than controls (Figs.2c and d). Western blotting for CLAMP
346 in *clamp* null larvae brains verified the absence of CLAMP protein in L3 brains (Fig.2e).
347
348 ***Loss of CLAMP disrupts brain development***
349
350 To evaluate CNS development in *clamp null* mutants, we focused on the mid/late L3 stage (~120 hours
351 after larval hatching (ALH)), because the *clamp* mutants die during late L3/early pupa stages. To gain
352 temporal insight, we also examined early L3 larvae brains. The overall morphology of the CNS, as observed
353 with DAPI staining, is different between nulls and controls (Figs.3a and e). As neural development
354 progresses through the larval stages, the neuroepithelial (NE) cells of the optic lobe (OL) start to
355 differentiate into neuroblasts (NBs), which will subsequently divide to give rise to neurons and glia
356 (CONTRERAS *et al.* 2019a). We observed that the *clamp* null OL is profoundly reduced in size. Specifically,
357 the clamp *null* OL neuroepithelia at 120 hours ALH resemble the control neuroepithelia at 72 hours ALH
358 (i.e., early L3) (Figs. 3a, b, e and f). Similarly, the *clamp* mutant central brain (CB) of the mid/late L3, has
359 an underdeveloped morphology and resembles the early control CB (Figs.3f and a).
360

361 Next, we examined NSCs in *clamp* null and control brains using an antibody against Deadpan (Dpn), which
362 labels all NSCs. Full z-stacks of the Dpn-positive NSCs in early and mid/late L3 brains (Figs. 3c, d, g and
363 h), revealed that in the *clamp* null, the development of NBs, both in the CB and OL, is considerably delayed
364 from the early L3 stage and remains so until the mid/late L3 stage when the animals die. The OL NB
365 population is greatly affected as the area containing Dpn-positive NSCs is much smaller in *clamp* nulls than
366 controls in mid/late L3 brains (Figs 3d and h, dashed outlines). These observations suggest that the deficits
367 observed in L3 *clamp* null brains may be due to an earlier arrest of NEs, resulting in the generation of fewer
368 NSCs. Comparison of early L3 *clamp* heterozygotes ($clamp^{+/-}$) and *clamp* null brains indicates that a single
369 copy of the *clamp* gene is sufficient to maintain the overall morphology of the developing OL
370 (Supplementary Fig. 1).
371
372 ***Developmental transcriptomic analysis of clamp null mutants reveals a role for CLAMP in nervous***
373 ***system development***
374
375 The neurodevelopmental deficits observed in the larval *clamp* null mutant brain suggest that the function
376 of CLAMP initiates earlier than the L3 stage. CLAMP is a ubiquitously-expressed TF, and is present
377 throughout the nervous system from early embryonic stages due to the deposition of maternal transcripts
378 into the egg (RIEDER *et al.* 2019) (Fig.1a). Each neurodevelopmental stage is characterized by unique
379 transcriptomic events controlled by specific TF factor networks (KONSTANTINIDES *et al.* 2018). Thus, to
380 understand how CLAMP regulates nervous system development on the transcriptomic level, we conducted
381 RNA-sequencing at the following key developmental stages in *clamp* null mutants: A) late stage embryos
382 (16-18 hours), a time point where neurogenesis pauses (HAKES *et al.* 2018) and most NBs enter quiescence
383 (Fig.4a); and B) mid/late L3 stage brains (Fig.4b), when neuronal and glial cell production are at their
384 maximum (AVET-ROCHEX *et al.* 2012). The selection of the specific embryonic time point was based on
385 studies by Haussmann et al. (2008, 2010), where *clamp* was identified as a functional interactor of
386 *embryonic lethal abnormal vision* (*elav*)and *erect wing* (*ewg*), in 16-18 hour embryos (HAUSSMANN *et al.*

387 2008; HAUSSMANN AND SOLLER 2010a). Both *elav* and *ewg* are critical to nervous system development
388 (ROBINOW AND WHITE 1988; DESIMONE AND WHITE 1993), further underscoring a potential role of
389 CLAMP in the process. To control for non-specific transcriptional changes due to other mutations that
390 could be in the genetic background, we used the *CLAMP* rescue line as a control (URBAN 2017). In the
391 *CLAMP* rescue line, *clamp* is inserted into an attP site under the control of the endogenous promoter.
392
393 Analysis of our transcriptomic data revealed that many genes were significantly differentially expressed
394 (DEGs) both in the embryo and the L3 brain (padj ≤ 0.05, Figs 4a-c). Interestingly, a large proportion of
395 DEGs were shared between embryo and L3 brain data sets (Fig.4c). The embryo dataset contains 5917
396 DEGs (padj ≤ 0.05 and Supplementary Table 1a), while the L3 contains 4465 DEGs (padj ≤ 0.05 and
397 Supplementary Table 2a). Of these DEGs, 2363 are shared between the two stages representing 40% of the
398 embryonic DEGs and 53% of the L3 DEGs. The size of this shared DEGs dataset supports the hypothesis
399 that *clamp* regulates gene networks controlling neurodevelopment form embryonic to L3 stages.
400
401 Analysis of the transcriptomic data revealed that a great number of genes was significantly and differentially
402 expressed (DEGs) both in the embryo and the L3 brain (padj ≤ 0.05, Figs 4a-c). Interestingly, a large
403 proportion of the DEGs was shared between the embryo and the *clamp* null L3 brain (Fig.4c). Accordingly,
404 the embryo dataset contains 5917 DEGs (padj ≤ 0.05 and Supplementary Table 1a), whereas the L3, 4465
405 DEGs (padj ≤ 0.05 and Supplementary Table 2a). Of these DEGs, 2363 are shared between the two stages
406 representing 40% of the embryonic DEGs and 53% of the L3 genes. The size of this shared DEGs dataset,
407 support the hypothesis that *clamp* deletion results in major changes in gene networks controlling
408 neurodevelopment, beginning form the embryonic stage and propagated through the L3 stage.
409
410 GO analysis revealed statistically significant enrichment for developmental/stem cell-related GO
411 categories, including neural development, at both the embryonic and larval developmental stages (Figs.4d,
412 e). Due to the neurodevelopmental defects in the *clamp* null mutant, we then specifically mined our

413 expression data for differential expression of genes that are implicated in cell cycle attributes, nervous
414 system development and neural stem cell biology. Enrichment was also observed for GO categories
415 involving metabolic pathways. This is interesting as post-embryonic neurogenesis is largely orchestrated
416 by signals originating from nutrient availability and insulin signaling (BRITTON AND EDGAR 1998; BAILEY
417 *et al.* 2015; GALAGOVSKY *et al.* 2018).
418
419 Functional analysis of the embryonic DEG dataset revealed highly statistically significant enrichment in
420 categories such as cell cycle regulation, cell cycle checkpoints, mitotic cell cycle phase transition,
421 neurogenesis and nervous system development, metabolic processes, synaptic development and signaling
422 (Supplementary Table 1b). We focused our analysis on two major highly enriched GO categories: i). *Cell*
423 *Cycle Regulation* [GO:0051726, padj: 6.22E-11] and ii). *Nervous System Development* [GO:0007399, padj:
424 4.32261E-05].
425
426 For the *GO:0051726 -Cell Cycle Regulation* category (Supplementary Table 1c), functional analysis of
427 identified DEGs suggests specific roles, including in G2/M transition of the mitotic cell cycle, regulation
428 of chromosome segregation, cell cycle G1/S phase transition, negative regulation of nervous system
429 development and of insulin signaling (Fig.4d).
430
431 Expression of *elav,* an RNA-binding protein and master regulator of neural development, was increased in
432 the absence of CLAMP [L2FC: 0.44; padj: 0.045]. ELAV regulates the expression of *ewg* and both are
433 critical for nervous system development, and neuronal maturation (ZAHARIEVA *et al.* 2015). Haussmann et
434 al. (2008, 2010) (HAUSSMANN *et al.* 2008; HAUSSMANN AND SOLLER 2010b) reported that *clamp* along
435 with a group of nine functionally-related genes which includes *groucho,* another critical developmental
436 regulator (TURKI-JUDEH AND COUREY 2012), are positively regulated by EWG and restrict synaptic growth
437 (Table 1). Notably, 9 out of 10 DEGs regulated by EWG are also DEGs in the *clamp* null embryos.

438 Therefore, it is possible that a synergistic relationship exists between the CLAMP and ELAV/EWG
439 pathways, in which they mutually regulate each other's expression to ensure proper brain development.
440
441 Meta-analysis of the *GO:0007399: Nervous System development* category (Supplementary Table 1d),
442 revealed strong enrichment in the sub-categories of neurogenesis and central nervous system, visual system
443 development, and glial cell development and differentiation (Fig.4e). Several DEGs critical for neural
444 development and NSC biology were identified: *Notch* [L2FC: -0.5, padj: 0.01], *lola* [L2FC: -0.6, padj:
445 0.004], and components of the Brahma chromatin remodeling complex such as *moira* [L2FC: -1.019, padj:
446 6.21E-05] (NEUMÜLLER *et al.* 2011; JANSSENS *et al.* 2014; SOUTHALL *et al.* 2014). Importantly, many
447 DEGs are part of specific TF networks that regulate different aspects of neural stem cell renewal identified
448 by Neumuller et al. (2011): *Su(z)12, Su(var)2-10*, the Hdac1 *Rpd3* [L2FC: -0.93, padj: 0.0004], and *lola*.
449 Notch signaling is critical for the balance between proliferation and differentiation in NSCs and maintains
450 the balance between the symmetrically and asymmetrically dividing stem cell pools in the optic lobe
451 (EGGER *et al.* 2010), neuroblast selection and delamination (AREFIN *et al.* 2019) and is a key regulator of
452 asymmetric divisions throughout the nervous system (CONTRERAS *et al.* 2018; HAKES AND BRAND 2019).
453
454 Furthermore, additional DEGs in the *Nervous System development* GO category are: 1) *polo, aPKC, par6,*
455 *pins, aurA* and *baz,* all components of the Par-complex which regulates asymmetric neuroblast divisions;
456 2) *PCNA, RFC38, dacapo,* and *Reptin* (part of the Tip60 complex), which participate in the molecular
457 network controlling cell polarity, asymmetric NSC division and cell fate (NEUMÜLLER *et al.* 2011); 3)
458 *CSN1b, CSN4* and *non-stop* which are implicated in lamina glia cell migration and optic lobe development
459 (WEAKE *et al.* 2008).
460
461 Categorization of the embryonic DEGs allowed us to identify potential pathways in which CLAMP is likely
462 to regulate target genes. Overall, lack of CLAMP results in dysregulation of three inter-dependent gene/TF

463 networks: 1) neurogenesis/gliogenesis; 2) cell cycle/asymmetric division; and 3) neuronal
464 arborization/synaptogenesis.
465
466 **Transcriptomic analysis of overlapping embryo and L3 *clamp* null DEGs implicates CLAMP in**
467 **regulating embryonic and post-embryonic neurogenesis.**
468
469 The transition from the embryonic to the post-embryonic stage is accompanied by many physiological
470 changes with the most notable being the introduction of feeding which brings about a cascade of metabolic
471 signal that induces activation of quiescent NSCs and neurogenesis. Comparison of the *clamp* null embryo
472 and L3 mRNA-seq results revealed that many DEGs were shared amongst the two stages (2363 DEGs)
473 (Fig.4b). Meta-analysis of the top two GO categories arising from the DEGs shared between embryos and
474 L3 DEGs revealed that identified genes have key roles in nervous system development, neurogenesis, and
475 mitotic cell cycle, suggesting continuing roles in neural development pre- and post-embryonically.
476
477 The fact that cell cycle-related categories were enriched in our transcriptomic analysis is interesting because
478 CLAMP maintains its expression in L3 proliferating NSCs and co-localizes with PCNA (Figs.1i and j),
479 which has critical roles in the cell cycle (KURKI *et al.* 1986). The expression of *pcna* is downregulated in
480 both developmental stages (*clamp* null embryo L2FC: -1.692 and L3 larva L2FC: -0.824, Supplementary
481 Tables 1a and 2a) along with other cell cycle regulators/chromosome dynamics factors such as *AurB*, *atms*
482 and *baz*, suggesting that CLAMP may regulate cell cycle progression and dynamics directly at a subset of
483 its targets.
484
485 **CLAMP regulates genes controlling NSC attributes, glia development and function**
486
487 The L3 stage encompasses a dramatic shift in the establishment of the nervous system. A plethora of
488 signaling pathways, including metabolic signals stimulated by larval feeding (CHELL AND BRAND

489 2010)(BRITTON AND EDGAR 1998; LANET *et al.* 2013), are integrated at the L3 stage to allow NSCs to
490 promote maturation of the nervous system. Consistent with this shift in NSC function, GO analysis of the
491 L3 DEGs (Supplementary Table 2b) revealed an enrichment in several broad categories, including
492 neurogenesis, mitotic DNA replication, and neuroblast differentiation. We find expression changes in many
493 genes critical for nervous system development, including those in the following categories: 1) neuroblast
494 attributes; 2) cell cycle dynamics; 3) glial cell development; 4) optic lobe development; 5) ecdysone &
495 insulin signaling dynamics; 6) lipid metabolism; 7) CLAMP-related interactors; 8) Synapse function &
496 structure.
497
498 Next, we classified DEGs as downregulated or upregulated in the *clamp* null mutant (downregulated vs.
499 upregulated, Tables 2 and 3, respectively). Downregulated genes are putatively targets activated by
500 CLAMP in wild-type animals. These genes could be classified into the following categories: 1) *NSC*
501 *attributes* (cell-cycle progression, cell polarity, and survival); 2) *control* of *NSC evolution/differentiation*;
502 3) *regulation of gliogenesis*; 4) *optic lobe development-specific*. In contrast, upregulated genes that are
503 putatively repressed by CLAMP are part of the following categories: 1) *lipid metabolism/promoting*
504 *mobilization of lipids*; 2) *ecdysone and insulin signaling in glia cells*; 3) *pro-arborization/synapse*
505 *formation and function*; 4) *pro-neural/suppression of proliferation*. Based on these data, we hypothesized
506 that loss of *clamp* leads to deficits in neural stem cell attributes and promotes changes that lead to the
507 precocious acquisition of a neuronal fate at the expense of gliogenesis. Our expression data also suggest
508 that loss of *clamp* may cause concomitant activation of lipid metabolism/mobilization as a compensatory
509 response from the stem cell-niche. Of great interest, we observed a prominent and strong downregulation
510 in genes orchestrating OL development such as *eya, tll, dac* and *optix* (See Table 2 and Supplementary
511 Tables 2d and Figs.4b). The downregulation of OL development master regulatory genes in the absence of
512 *clamp* aligns with the greatly reduced size of the OL (Fig.3) in the L3 *clamp* null mutants. Collectively,
513 these data are consistent with a critical role for CLAMP in the regulation of OL NSCs compared with the
514 rest of the brain.

515

516 ***CLAMP binds major neurodevelopment genes***

517

518 To evaluate the possibility of direct regulation of DEGs by CLAMP, we determined where CLAMP binding
519 sites are present upstream of target genes using FIMO analysis (GRANT *et al.* 2011). Previously
520 characterized CLAMP binding motifs were used for this analysis (KAYE *et al.* 2018). Interestingly, genes
521 that contain putative CLAMP binding sites and are dysregulated in *clamp* nulls in both the embryonic and
522 L3 stages include : 1) the important proliferation/mitosis regulators *bazooka (baz), separation anxiety* (*san)*,
523 a N-terminal acetyltransferase required for mitotic chromosome segregation (RIBEIRO *et al.* 2016), *cyclin*
524 *dependent kinase 7* (*cdk7*) vital for mitosis (LAROCHELLE *et al.* 1998), *PCNA* and *Notch*; 2) *sobremesa*
525 (*sbm*) an SLC7 amino acid transporter expressed in glia and regulating brain development *via* ecdysone
526 signaling(GALAGOVSKY *et al.* 2018); and *Negative elongation factor E* (*nelf-E*) which is a known interactor
527 of CLAMP (URBAN 2017) (Fig.4f, Embryo and L3 panel).

528

529 Developmental stage-specific genes that contain putative CLAMP binding sites include: A) <u>*Embryo stage*</u>:
530 *anaphase promoting complex subunit 7* (*APC7*)*; pontin (pont)* which is part of the TIP60 complex which
531 regulates NSC attributes*; aurora A (aurA)* a kinase regulating asymmetric protein localization and thus
532 required for NSC proliferation (LEE *et al.* 2006)*; extra sex combs (esc)*, a component of the PRC2 complex
533 which regulates NSC proliferation and neural development (CURT *et al.* 2019) and *fruitless (fru)*, implicated
534 in the formation of axonal projections in the embryonic CNS (SONG *et al.* 2002) (Fig.4e, Embryo panel).
535 B) <u>*L3 stage*</u>: Even more interesting during the L3 stage (Fig.4f, L3 panel), CLAMP binding motifs are
536 found in *gcm,* an essential regulator of glial development*; glass bottom boat* (*gbb*) which regulates both
537 NB proliferation and surface glia survival; tailless (*tll),* a key regulator of optic lobe development and
538 *anaplastic lymphoma kinase (Alk)* which is implicated in cell cycle regulation and NSC proliferation; and
539 *Dichaete* (*D*), a TF regulating neuronal fate in the OL.

540

541 ***CLAMP directly binds and regulates Tailless and Notch***

542

543 To further examine and validate which of the FIMO-identified CLAMP binding targets have been
544 experimentally-confirmed, thus provide the basis for their direct binding and regulation by CLAMP, we
545 mined available embryonic 0-24 hour CLAMP ChIP-seq data generated by modENCODE (CONSORTIUM
546 *et al.* 2010) and L3 whole larval data (KUZU *et al.* 2016) using the Integrative Genomics Viewer (IGV)
547 (ROBINSON *et al.* 2011). This analysis revealed that CLAMP has been experimentally been validated to
548 directly bind to *baz*, *Notch and, Nelf-E,* the latter of which serves as a positive control to our results as it is
549 a validated target of CLAMP (URBAN 2017) (Fig.4g). Importantly, CLAMP directly binds and regulates
550 *Tll* expression (Fig.4g), which indicates that the defects in OL development seen in the *clamp* null mutants
551 is due to downregulation of *tll* expression in the absence of CLAMP.

552

553 To further assess direct regulation by CLAMP, we quantified CLAMP binding to DEGs in both our data
554 sets compared to a control gene set of neuronally expressed genes. In support of a direct regulatory role
555 for CLAMP at a subset of its target genes, we found that genes that are downregulated in *clamp* nulls show
556 higher average read depth around the TSS (Fig. 4h) and have a greater binding frequency, particularly in
557 larvae.

558

559 ***CLAMP promotes NSC proliferation and prevents precocious neurogenesis***

560

561 Our transcriptomics analysis results demonstrate that CLAMP is exerting direct control on neural
562 development by directly regulating the transcription of key effectors that function in multiple processes
563 including asymmetric cell division, cell cycle and optic lobe development (DANIEL *et al.* 1999; DAS AND
564 BHADRA 2020), both in embryos and larvae (Figs.4f, g). Importantly, we observed a marked decrease in
565 glial-development and cell cycle dynamics genes in the absence of CLAMP (Table 2).Therefore, we

566 hypothesized that lack of CLAMP disturbs the balance between neuronal and glia formation through the
567 L3 stage, by impinging neural stem cell proliferation, especially in the OL.
568
569 To test our hypothesis, we evaluated mid-late L3 brains for proliferating NSCs using the S-phase marker
570 EdU, the NSC marker Dpn and a quantification approach introduced by Kanai et al.(KANAI *et al.* 2018) in
571 which the superficial layers of the brain are evaluated. We chose this approach due to the importance of
572 superficial glia in the overall biology of neuroblasts and used it throughout our study. Consistent with our
573 initial observations (Fig.3), the OL in *clamp* null larvae brains was dramatically reduced in size compared
574 to controls, and both the CB and OL contained fewer proliferating NSCs ($EdU^{+}Dpn^{+}$, Figs.5a and c and
575 Supplementary Figs.2 a, b). Quantification of total proliferating NSCs (EdU+) from the superficial layers
576 of the brain (KANAI *et al.* 2018), showed a dramatic ~90% reduction compared to controls (Fig. 5e).
577 Moreover, we observe an overall reduced number of proliferating cells compared to controls, suggesting a
578 reduced proliferation of stem cells and/or change in cell cycle dynamics in the absence of CLAMP (EdU+
579 Fig.5e).
580
581 Genes encoded by many pro-neural TFs are upregulated in the absence of CLAMP (Table 3), in addition
582 to TFs that promote cell cycle regulation in proliferating stem cells. Specifically, in the L3 *clamp* null brain
583 *dpn*, which regulates NSC proliferation, was significantly downregulated (Table 2; L2FC: -0.665, padj:
584 0.00245). The combination of reduced *dpn* transcript levels and the reduced numbers of proliferating NSCs
585 in the *clamp* null brains suggest that CLAMP may regulate NSC differentiation.
586
587 The TF Prospero (Pros), acts as a master regulator driving the decision of stem cells to either self-renew or
588 differentiate (CHOKSI *et al.* 2006), with nuclear Pros signaling the initiation of neuronal differentiation
589 (KNOBLICH AND JAN 1995; CHOKSI *et al.* 2006). Thus, to evaluate changes in neuronal production in the
590 *clamp* null brain we performed Pros immunostaining. We found that the *clamp* null brain contained more
591 clusters of nuclear Pros immunostaining than matched controls, thus indicating a rapid change in NSC cell

592 fate attributes (COLONQUES *et al.* 2011) (Figs.5b and d, arrows indicate Pros+ clusters). Interestingly, while
593 the total number of NSCs in the *clamp* null brain was reduced by approximately 70% (Dpn^+, Fig.5f), Pros+
594 cell numbers were increased by approximately 70% ($Pros^+$, Fig.5f), indicating that stem cells are acquiring
595 a precocious neuronal fate. The reduction in NSCs is particularly evident in the OL, where very few Dpn+
596 cells were observed, contrary to a widespread presence of Pros+ cells ~~were present~~ (Figs.5a-d, outlines in
597 Figs.5b and d indicate the OL). Pros, acts a transcriptional repressor of self-renewal genes and induces
598 differentiation (CHOKSI *et al.* 2006; LAI AND DOE 2014). While a significantly higher number of cells have
599 nuclear Pros (Pros+, Sup.Fig.2c) in the *clamp* null brains, most of these cells have not incorporated EdU
600 (Pros+EdU-, Sup.Fig.2c). In combination with the finding that in the *clamp* null brain, a lower number of
601 cells incorporate EdU within the pulse window, and thus a smaller number of NSCs are actively
602 proliferating (Fig.5e), the Pros immunostaining suggests that in the absence of CLAMP, NSCs undergo
603 fewer cell division cycles and/or precociously exit the cell cycle to acquire a differentiated fate.
604
605 To further evaluate changes in the neuronal pool of cells, we performed Elav staining to label neurons
606 (ROBINOW AND WHITE 1988), which revealed that *clamp* null brains contain a higher density of $Elav^+$
607 clusters compared to controls (Figs.5g and h). However, even though the overall Elav+ cluster density
608 increased the $Elav^+$ zone in the OL was reduced compared to controls (Figs. 5g and h, yellow outlines).
609 Immunostaining with the apoptotic marker Dcp1 revealed increased and specific presence of $Dcp1^+$ nuclei
610 in the OL in *clamp* nulls, compared to the controls which instead, had more widespread apoptosis (Figs. 5i
611 and j). Moreover, in more dorsal optical sections large Dcp1+ clusters were visible in the medulla and
612 lamina area (Supplementary Figs.3a and b). These results suggest that in the absence of CLAMP a pro-
613 differentiation pathway is activated in stem cells at the expense of their self-renewal which especially
614 impacts the OL.
615
616 ***Expression of the optic lobe development master regulator Tailless, is severely reduced in the clamp null***
617

618 Our results thus far revealed a direct control of the key OL development gene, *tailless* by CLAMP,
619 culminating in a severely underdeveloped OL in the *clamp* null and downregulation of *tll* in the *clamp* null
620 (Fig.4 and Fig.6). Interestingly, in *tll* knockdown animals, the OL is severely underdeveloped or absent,
621 OL neurogenesis is affected and OL neuroblasts undergo increased apoptosis, as seen in the *clamp* null OLs
622 (GUILLERMIN *et al.* 2015). To examine whether the *clamp* null OL phenotype can be attributed to a loss of
623 the Tll protein, we performed immunofluorescence. This approach revealed a consistency between the
624 dramatic reduction in the *tll* transcript identified by mRNA-seq and the protein, with the latter being almost
625 absent in the OL neuroepithelium (Fig.6d). *tll* expression is required for the survival of the OL NSCs since
626 its absence leads to apoptosis (GUILLERMIN *et al.* 2015), which is in agreement with the increased and
627 specific cell-death we observed in the OL region (Figs. 5i and j and Supplementary Figs.3a and b).
628 Furthermore, it highlights that CLAMP has a direct control in OL development through binding to the *tll*
629 promoter to regulate *tll* expression.
630
631 ***Lack of CLAMP results in reduction in number of surface glia***
632
633 OL development is highly dependent on glia-neuron interactions because glia form a supportive niche for
634 neural stem cells to function (PEREANU *et al.* 2005; RAMON-CAÑELLAS *et al.* 2018). Furthermore,
635 neuroepithelial cells of the OL, give rise to hundreds of precursor/progenitor cells of different lineages,
636 including neuroglioblasts and glial progenitor cells. For the lineage diversification to take place an intricate
637 temporal expression of fate-determining TFs occurs in the precursor cells, including *Notch* and *Tll,* both of
638 which are under direct CLAMP control (Fig.4g). In OL medulla NBs, Tll is expressed in the oldest NBs
639 which go on to generate neuronal progeny or express *glia cells missing (gcm)* and gradually turn off *Tll* to
640 express *Repo* as glial cells (LI *et al.* 2013).
641
642 Our transcriptomic analysis supports the hypothesis that lack of CLAMP promotes neuronal differentiation
643 at the expense of gliogenesis from the late embryo stage. Therefore, the defects observed in OL

644 development of the L3 *clamp* null could be attributed to a combination of deficits in gliogenesis, precocious
645 neurogenesis as a result of altered *Tll and/or Notch* expression. It was recently shown that surface glia (SG)
646 are crucial for NB proliferation (KANAI *et al.* 2018), an interplay which involves niche and autocrine
647 signaling. Specifically, SG regulate NSC proliferation *via* the secretion of the proteoglycan Dally-like,
648 (Dlp); 2) Stem cells secrete the BMP-ligand Glass bottom boat (Gbb) which regulates their proliferation
649 and both the stem cell and SG survival. Interestingly, the *gbb* gene contains CLAMP-binding motifs
650 (Fig.4f) and is downregulated in the *clamp* null L3 brains (Supplementary Table 2d). Furthermore, we
651 observed enrichment of the BMP-signaling GO category in the *clamp* null (Fig.4d). Therefore, a loss of the
652 dynamic interplay between SG and NSCs resulting from the altered expression of key fate-determining
653 TFs, *Tll* and *Notch* in the absence of CLAMP could also contribute the deficits in the *clamp* null brain.
654
655 To test this hypothesis, we first examined whether a change in SG numbers is seen in the *clamp* null. We
656 used the glia-specific marker Repo (XIONG *et al.* 1994b; YUASA *et al.* 2003) to mark glial cells, and
657 quantified SG in L3 brains using the approach by Avet-Rochex et al. (2012) (AVET-ROCHEX *et al.* 2012).
658 This revealed a ~25 % reduction in SG number in the *clamp* null, compared to the control (Figs.7 a-d).
659 Additionally, the distribution and numbers of glial cells throughout the brain (Supplementary Figs. 3c and
660 d) and especially of the OL and the lobula plug was altered in terms of topological organization
661 (Supplementary Figs. 3e and f). Overall, these data suggest that CLAMP regulates gliogenesis and glia
662 distribution especially in the OL.
663
664 To determine if the effect on SG number was due to the lack of CLAMP in glia specifically, we used the
665 GAL4-UAS system to induce *clamp*-RNAi knock down (KD) using the glia-specific driver, *repo-GAL4*
666 *(XIONG et al. 1994a)*. Interestingly, we find that in the *repo>clamp RNAi* brains, the number of SG was
667 reduced to a similar extent as in the *clamp* nulls (Repo+ cells, ~30% reduction, Figs. 7a-d). To determine
668 whether glia-specific or neuronal-specific *clamp* depletion has differential effects on the proliferation
669 (EdU+) and the number of NSCs (Dpn+ cells), we also performed neuronal *clamp* KD by crossing to an

670 *elav-GAL4* fly line (LIN AND GOODMAN 1994). Comparison with the data we already obtained from the
671 *clamp* null and control brains (see Figs.5e and f) revealed that *clamp* KD in neuronal lineages did not result
672 in significant changes either in EdU+ or Dpn+ cells, while glia-specific *clamp* KD caused a reduction in
673 the number of total proliferating cells (EdU+ cells, ~15% reduction compared to control). Thus, while glial
674 *clamp* KD results in the same amount of reduction in Repo+ SG number as in the *clamp* null, the effect on
675 proliferating NSCs is smaller compared to the null. This suggests that downregulation of glial CLAMP
676 mainly affects the proliferation of glia-producing NSCs likely *via* both cell autonomous mechanisms (e.g.,
677 reduction in Dpn+ gliogenic NSCs) and *via* non-cell autonomous mechanisms (regulation of proliferation
678 by niche glia), although it does not recapitulate the full phenotype seen in the *clamp* null leaving room for
679 additional mechanisms.
680
681 In summary, our results suggest that CLAMP controls NSC stemness, proliferation and lineage output,
682 especially in the OL, by directly regulating the expression of key TFs such as *Notch* and *Tailless,* and by
683 affecting neural stem cell niche homeostasis. Ultimately, lack of CLAMP leads to imbalance in neuronal
684 over glial generation and leads to precocious differentiation of neural stem cells.
685
686 **Discussion**
687
688 The understanding of the gene regulatory mechanisms by which neural stem cells function to ultimately
689 build the brain is critical to provide insight into normal. Signaling relays originating from the stem niche
690 play an instructive role in the neurogenetic process, and highlight the fact that the environmental context
691 acts synergistically with intrinsic developmental signals (SCADDEN 2006; SPEDER AND BRAND 2018). In
692 this study, we have defined a new role for the essential transcription factor, CLAMP, in nervous system
693 development and NSC-niche interactions, especially in optic lobe development. We show that CLAMP
694 positively directly regulates *Notch* and *Tailless*, which regulate NSC stemness, proliferation and progeny
695 output, while *Tailless* is a master regulator of OL development. The multilayered control of CLAMP over

696 NSC function is evidenced in *clamp* null brains, where the OL is severely underdeveloped, niche glial cell
697 generation is reduced in favor of precocious neurogenesis, while concurrently the niche protective
698 mechanisms are overactivated. Furthermore, lack of *clamp* affects the expression of key NSC
699 proliferation/division genes such as *baz*. In summary, our study reveals that CLAMP regulates brain
700 development *via* cell-intrinsic and NSC niche-dependent mechanisms that involve niche glia.
701
702 The formation of the OL is profoundly impaired in *clamp* null mutants, a phenotype accompanied by
703 reduction of EdU^+ NSCs (Figs.5a-d). We also observed increased numbers of $Pros^+$ cells in the null OL
704 (Figs. 5b and d, outlined area) and throughout the brain, consistent with lack of CLAMP promoting a
705 neurogenic over a gliogenic fate. While glial *clamp* KD results in a partial reduction in the number of
706 proliferating NSCs (EdU^+, Fig.6e), it does not affect the number of Dpn^+ NSCs/neuroblasts. These results
707 suggest an effect on the Dpn^- progeny of the NSCs, such as the ganglion mother cells (GMCs) and common
708 progenitor cells (CPCs) of the OL. This is an intriguing scenario as CPCs divide asymmetrically to generate
709 Lawf precursor cells and glial precursor cells (GPCs); glial *clamp* KD resulted in the approximately the
710 same reduction in Repo+ glial cells, as seen in the *clamp* null. Although, Pros+ cells were not counted in
711 the glial *clamp* KD brains, evaluation of the mean signal intensity of the Pros channel suggested an
712 increased signal compared to the control (not shown) and suggesting the lack of CLAMP alters the balance
713 between neuronal and glial-progenies at the precursor level. Also, it is possible that there are changes in the
714 cell cycle kinetics that cause fewer NSCs to be actively proliferating. This possibility is consistent with the
715 GO analysis which identified genes involved in cell cycle kinetics/transitions (Fig4.c).
716
717 Moreover, as CLAMPs' specific role in OL development is evidenced by the fact that CLAMP directly
718 binds and positively regulates *tll* expression, which is also downregulated both at the transcript and protein
719 levels in the OL, in the absence of CLAMP (Fig.4). Furthermore, other transcription factors critical for OL
720 neurogenesis such as *eya, dac* and *optix* are downregulated in the *clamp* null mutant brains (see Table 2).
721

722 In the post-embryonic nervous system, *gcm* and *gcm2* are expressed in OL NSCs destined both for glia and
723 neuron generation which they regulate *via* downstream mechanisms involving Dachshund (Dac)(CHOTARD
724 *et al.* 2005). The expression of g*cm, gcm2* and *dac* is reduced in the *clamp* null (Table 2). Moreover, both
725 *gcm* and *gcm2* transcript levels were greatly reduced in the *clamp* null L3 brain, while *gcm* contains CLAMP
726 binding sites (Fig.4e). The OL contains a special population of NSCs, the common progenitor cells (CPCs),
727 which generate both glia precursor cells (GPCs) and neurons (Lawfs), under the control of Notch signaling
728 (CHEN *et al.* 2016). Moreover, Notch is a key regulator which maintains the balance between
729 symmetric/self-renewing and asymmetric NSCs divisions; loss of Notch function promotes precocious
730 differentiation and premature neurogenesis (EGGER *et al.* 2010). In the absence of CLAMP, *Notch* is at
731 least two-fold downregulated both in the embryonic and L3 stages (Supplementary Table 1a and Table 2),
732 and we determined that Notch has a CLAMP binding site and is a direct target for CLAMP (Figs.4f and g).
733 Overall, our data support a model in which CLAMP functions upstream of *Notch* and *Tll* signaling, which
734 it directly binds, and regulates NSC proliferation and differentiation in the OL.
735
736 Neural development and NSC function are intricately linked to niche glia and depend on support and
737 nutrition from surface glia *via* Gbb-Dlp signaling, which sustains NSC proliferation and survival but also
738 ensures the survival of surface glia (KANAI *et al.* 2018). Thus, there is an interdependency between NSCs
739 and niche glia, ensuring overall homeostasis in the stem cell niche. In *clamp* null and *repo>clamp* RNAi
740 larvae brains, surface glia numbers are reduced to the same extent indicating that lack of glial CLAMP
741 affects gliogenesis (Fig.7d). Furthermore, the glial master gene, *gcm,* contains CLAMP binding motifs and
742 is significantly downregulated in the *clamp* null brain, indicating that CLAMP may directly regulate
743 gliogenesis through *gcm*-related mechanisms (Fig.4f). Supportive of a glial role for CLAMP is the fact that
744 glial-specific *clamp* KD by *repo*-GAL4, resulted in specific reduction of SG cells, to the same extend seen
745 in the *clamp* null. In contrast, a neuronal specific *clamp* KD (*elav> clamp* RNAi) did not affect NSC
746 proliferation, number or, glial cell number (Fig.6). A small reduction in cycling cells (~15%, EdU+) was
747 observed in *repo>clamp* RNAi conditions compared to a massive 85% reduction in the *clamp* null brain.

748 This difference can be attributed to the fact that in the *repo>clamp* RNAi conditions, the reduction in *clamp*
749 levels will only take place after *repo* expression is established during terminal differentiation of glial cells,
750 and through direct induction by Gcm (YUASA *et al.* 2003).
751
752 In the future, it will be interesting to determine whether this reduction in glial cell number can be attributed
753 specifically to glia-producing cells in which *gcm* activity is still high and indicative of their proliferation
754 status. In the *clamp* null mutants, *clamp* is depleted before *repo* starts to be expressed and thus may result
755 in a greater impact on NSC proliferation and neuronal production in the OL because both *gcm* and *gcm2*
756 regulate glial and neuronal development in the OL via *Dac* (CHOTARD *et al.* 2005) which is also
757 downregulated in the *clamp* null brain (Table 2). Thus, it is possible if we used *gcm*-GAL4 to drive *clamp*
758 RNAi at earlier stages, we would unmask a greater effect both on NSC proliferation and NSC number.
759
760 We also observed that the *foxO* gene (Forkhead box, class O) is part of many of the cell cycle sub-categories
761 that we identified from GO analysis, including the *insulin signaling category*, which is a known target of
762 FOXO (KRAMER *et al.* 2003). FOXO belongs to a family of highly dynamic and conserved transcription
763 factors and regulates gene expression during processes such as apoptosis, cell-cycle transitions including
764 negative regulation of G1/S and G2/M (HUANG AND TINDALL 2007), both of which are highly enriched in
765 our GO analysis. Overexpression of FOXO during larval development results in reduction both in cell size
766 and number in the developing eye (KRAMER *et al.* 2003). In addition, it was shown that FOXO affects the
767 temporal sequence and cell fate specification in a subset of olfactory neurons in *Drosophila* (WEI *et al.*
768 2019). Interestingly, in the *clamp* null embryo the *foxO* transcript is upregulated (L2FC: 0.46846,
769 padj:0.000283, Supplementary Table 1a). Therefore, it is possible that some of the phenotypic effects that
770 we observed in the *clamp* null mutant are also related to dysregulation of *foxO* gene expression (KRAMER
771 *et al.* 2003; WEI *et al.* 2019) .
772

773 *Clamp* is maternally deposited and its expression is high during the majority of embryogenesis (RIEDER *et*
774 *al.* 2017) (Fig.1a). While the persistence of maternal *clamp* was not specifically evaluated in late embryos,
775 CLAMP protein deposited by *clamp* heterozygous mothers persists beyond the embryonic stage and is
776 present in the histone locus body throughout the development of the larval salivary gland (RIEDER *et al.*
777 2017). Thus, it is possible that a trace amount of maternally deposited *clamp* could still be present at 16-18
778 hour embryos and reduces the strength of the zygotic *clamp* nulls phenotype compared with embryos that
779 are depleted of maternal CLAMP which die early in embryogenesis soon after zygotic genome activation.
780
781 Glial cells can arise from different mechanisms, either from dedicated glioblasts or from NBs that have
782 both glial and neuronal potential (BOSSING *et al.* 1996; BERNARDONI *et al.* 1999; SCHMID *et al.* 1999;
783 UDOLPH *et al.* 2001). Our results show that CLAMP regulates a transcriptional program which drives NSC
784 proliferation and differentiation *via* cell-intrinsic and niche-dependent mechanisms that involve
785 transcriptional regulation of *Tailless, Notch* and niche glia.
786
787
788
789
790
791
792
793
794
795
796
797
798

REFERENCES

Anders, S., P. T. Pyl and W. Huber, 2015 HTSeq—a Python framework to work with high-throughput sequencing data. Bioinformatics 31**:** 166-169.

Andrews, S., 2010 FastQC: a quality control tool for high throughput sequence data, pp. Babraham Bioinformatics, Babraham Institute, Cambridge, United Kingdom.

Arefin, B., F. Parvin, S. Bahrampour, C. B. Stadler and S. Thor, 2019 Drosophila Neuroblast Selection Is Gated by Notch, Snail, SoxB, and EMT Gene Interplay. Cell reports 29**:** 3636-3651. e3633.

Avet-Rochex, A., A. K. Kaul, A. P. Gatt, H. McNeill and J. M. Bateman, 2012 Concerted control of gliogenesis by InR/TOR and FGF signalling in the Drosophila post-embryonic brain. Development 139**:** 2763-2772.

Bailey, Andrew P., G. Koster, C. Guillermier, Elizabeth M. A. Hirst, James I. MacRae *et al.*, 2015 Antioxidant Role for Lipid Droplets in a Stem Cell Niche of Drosophila. Cell 163**:** 340-353.

Bernardoni, R., M. Kammerer, J.-L. Vonesch and A. Giangrande, 1999 Gliogenesis depends on glide/gcm through asymmetric division of neuroglioblasts. Developmental biology 216**:** 265-275.

Bertet, C., X. Li, T. Erclik, M. Cavey, B. Wells *et al.*, 2014 Temporal Patterning of Neuroblasts Controls Notch-Mediated Cell Survival through Regulation of Hid or Reaper. Cell 158**:** 1173-1186.

Bossing, T., G. Udolph, C. Q. Doe and G. M. Technau, 1996 The Embryonic Central Nervous System Lineages ofDrosophila melanogaster: I. Neuroblast Lineages Derived from the Ventral Half of the Neuroectoderm. Developmental biology 179**:** 41-64.

Britton, J. S., and B. A. Edgar, 1998 Environmental control of the cell cycle in Drosophila: nutrition activates mitotic and endoreplicative cells by distinct mechanisms. Development 125**:** 2149-2158.

Brown, J. B., N. Boley, R. Eisman, G. E. May, M. H. Stoiber *et al.*, 2014 Diversity and dynamics of the Drosophila transcriptome. Nature 512**:** 393-399.

Chell, J. M., and A. H. Brand, 2010 Nutrition-responsive glia control exit of neural stem cells from quiescence. Cell 143**:** 1161-1173.

825 Chen, Z., A. D. V. Rodriguez, X. Li, T. Erclik, V. M. Fernandes *et al.*, 2016 A unique class of neural
826 progenitors in the Drosophila optic lobe generates both migrating neurons and glia. Cell reports 15**:**
827 774-786.
828 Choksi, S. P., T. D. Southall, T. Bossing, K. Edoff, E. de Wit *et al.*, 2006 Prospero acts as a binary switch
829 between self-renewal and differentiation in Drosophila neural stem cells. Developmental cell 11**:**
830 775-789.
831 Chotard, C., W. Leung and I. Salecker, 2005 glial cells missing and gcm2 cell autonomously regulate both
832 glial and neuronal development in the visual system of Drosophila. Neuron 48**:** 237-251.
833 Colonques, J., J. Ceron, H. Reichert and F. J. Tejedor, 2011 A transient expression of Prospero promotes
834 cell cycle exit of Drosophila postembryonic neurons through the regulation of Dacapo. PLoS One
835 6**:** e19342.
836 Conard, A. M., N. Goodman, Y. Hu, N. Perrimon, R. Singh *et al.*, 2020 TIMEOR: a web-based tool to
837 uncover temporal regulatory mechanisms from multi-omics data. bioRxiv.
838 Consortium, m., S. Roy, J. Ernst, P. V. Kharchenko, P. Kheradpour *et al.*, 2010 Identification of functional
839 elements and regulatory circuits by Drosophila modENCODE. Science 330**:** 1787-1797.
840 Contreras, E. G., B. Egger, K. S. Gold and A. H. Brand, 2018 Dynamic Notch signalling regulates neural
841 stem cell state progression in the Drosophila optic lobe. Neural development 13**:** 1-11.
842 Contreras, E. G., J. Sierralta and C. Oliva, 2019a Novel strategies for the generation of neuronal diversity:
843 lessons from the fly visual system. Frontiers in Molecular Neuroscience 12**:** 452461.
844 Contreras, E. G., J. A. Sierralta and C. Oliva, 2019b Novel strategies for the generation of neuronal
845 diversity: lessons from the fly visual system. Frontiers in Molecular Neuroscience 12**:** 140.
846 Crews, S. T., 2019 Drosophila Embryonic CNS Development: Neurogenesis, Gliogenesis, Cell Fate, and
847 Differentiation. Genetics 213**:** 1111-1144.
848 Curt, J. R., B. Y. Salmani and S. Thor, 2019 Anterior CNS expansion driven by brain transcription factors.
849 Elife 8**:** e45274.

850 Dani, N., R. H. Herbst, N. Habib, J. Head, D. Dionne *et al.*, 2019 A cellular and spatial map of the choroid
851 plexus across brain ventricles and ages. BioRxiv**:** 627539.
852 Daniel, A., K. Dumstrei, J. A. Lengyel and V. Hartenstein, 1999 The control of cell fate in the embryonic
853 visual system by atonal, tailless and EGFR signaling. Development 126**:** 2945-2954.
854 Das, P., and M. P. Bhadra, 2020 Histone deacetylase (Rpd3) regulates Drosophila early brain development
855 via regulation of Tailless. Open Biol 10**:** 200029.
856 DeSimone, S. M., and K. White, 1993 The Drosophila erect wing gene, which is important for both neuronal
857 and muscle development, encodes a protein which is similar to the sea urchin P3A2 DNA binding
858 protein. Molecular and cellular biology 13**:** 3641-3649.
859 Egger, B., J. M. Chell and A. H. Brand, 2008 Insights into neural stem cell biology from flies. Philosophical
860 Transactions of the Royal Society B: Biological Sciences 363**:** 39-56.
861 Egger, B., K. S. Gold and A. H. Brand, 2010 Notch regulates the switch from symmetric to asymmetric
862 neural stem cell division in the Drosophila optic lobe. Development 137**:** 2981-2987.
863 Galagovsky, D., A. Depetris-Chauvin, G. Manière, F. Geillon, M. Berthelot-Grosjean *et al.*, 2018
864 Sobremesa L-type Amino Acid Transporter Expressed in Glia Is Essential for Proper Timing of
865 Development and Brain Growth. Cell reports 24**:** 3156-3166. e3154.
866 Gallaud, E., T. Pham and C. Cabernard, 2017 Drosophila melanogaster neuroblasts: a model for asymmetric
867 stem cell divisions, pp. 183-210 in *Asymmetric Cell Division in Development, Differentiation and*
868 *Cancer*. Springer.
869 Grant, C. E., T. L. Bailey and W. S. Noble, 2011 FIMO: scanning for occurrences of a given motif.
870 Bioinformatics 27**:** 1017-1018.
871 Graveley, B., G. May, A. Brooks, J. Carlson, L. Cherbas *et al.*, 2011 The D. melanogaster transcriptome:
872 modENCODE RNA-Seq data for dissected tissues. Retrieved from website: http://www.
873 modencode. org/Celniker. shtml.
874 Guillermin, O., B. Perruchoud, S. G. Sprecher and B. Egger, 2015 Characterization of tailless functions
875 during Drosophila optic lobe formation. Developmental Biology 405**:** 202-213.

876 Hakes, A. E., and A. H. Brand, 2019 Neural stem cell dynamics: the development of brain tumours. Current
877 Opinion in Cell Biology 60**:** 131-138.
878 Hakes, A. E., L. Otsuki and A. H. Brand, 2018 A newly discovered neural stem cell population is generated
879 by the optic lobe neuroepithelium during embryogenesis in *Drosophila melanogaster*.
880 Development 145**:** dev166207.
881 Hartenstein, V., and J. A. Campos-Ortega, 1984 Early neurogenesis in wild-typeDrosophila melanogaster.
882 Wilhelm Roux's archives of developmental biology 193**:** 308-325.
883 Haussmann, I. U., and M. Soller, 2010a Differential activity of EWG transcription factor isoforms identifies
884 a subset of differentially regulated genes important for synaptic growth regulation. Developmental
885 biology 348**:** 224-230.
886 Haussmann, I. U., and M. Soller, 2010b Differential activity of EWG transcription factor isoforms identifies
887 a subset of differentially regulated genes important for synaptic growth regulation. Dev Biol 348**:**
888 224-230.
889 Haussmann, I. U., K. White and M. Soller, 2008 Erect wing regulates synaptic growth in Drosophila by
890 integration of multiple signaling pathways. Genome biology 9**:** R73.
891 Hindle, S. J., and R. J. Bainton, 2014 Barrier mechanisms in the Drosophila blood-brain barrier. Frontiers
892 in neuroscience 8**:** 414.
893 Huang, H., and D. J. Tindall, 2007 Dynamic FoxO transcription factors. J Cell Sci 120**:** 2479-2487.
894 Janssens, D. H., H. Komori, D. Grbac, K. Chen, C. T. Koe *et al.*, 2014 Earmuff restricts progenitor cell
895 potential by attenuating the competence to respond to self-renewal factors. Development 141**:**
896 1036-1046.
897 Kanai, M. I., M.-J. Kim, T. Akiyama, M. Takemura, K. Wharton *et al.*, 2018 Regulation of neuroblast
898 proliferation by surface glia in the Drosophila larval brain. Scientific reports 8**:** 1-15.
899 Kaye, E. G., M. Booker, J. V. Kurland, A. E. Conicella, N. L. Fawzi *et al.*, 2018 Differential occupancy of
900 two GA-binding proteins promotes targeting of the drosophila dosage compensation complex to
901 the male X chromosome. Cell reports 22**:** 3227-3239.

902 Kaye, E. G., A. Kurbidaeva, D. Wolle, T. Aoki, P. Schedl *et al.*, 2017 Drosophila dosage compensation
903 loci associate with a boundary-forming insulator complex. Molecular and cellular biology 37**:**
904 e00253-00217.
905 Kim, D., B. Langmead and S. Salzberg, 2015 hisat2. Nature methods.
906 Kis, V., B. Barti, M. Lippai and M. Sass, 2015 Specialized cortex glial cells accumulate lipid droplets in
907 Drosophila melanogaster. PLoS One 10**:** e0131250.
908 Knoblich, J. A., and Y. N. Jan, 1995 Asymmetric segregation of Numb and Prospero during cell division.
909 Nature 377**:** 624-627.
910 Konstantinides, N., K. Kapuralin, C. Fadil, L. Barboza, R. Satija *et al.*, 2018 Phenotypic convergence:
911 distinct transcription factors regulate common terminal features. Cell 174**:** 622-635. e613.
912 Kramer, J. M., J. T. Davidge, J. M. Lockyer and B. E. Staveley, 2003 Expression of Drosophila FOXO
913 regulates growth and can phenocopy starvation. BMC developmental biology 3**:** 5.
914 Kurki, P., M. Vanderlaan, F. Dolbeare, J. Gray and E. Tan, 1986 Expression of proliferating cell nuclear
915 antigen (PCNA)/cyclin during the cell cycle. Experimental cell research 166**:** 209-219.
916 Kuzu, G., E. G. Kaye, J. Chery, T. Siggers, L. Yang *et al.*, 2016 Expansion of GA dinucleotide repeats
917 increases the density of CLAMP binding sites on the X-chromosome to promote Drosophila dosage
918 compensation. PLoS genetics 12**:** e1006120.
919 Lai, S.-L., and C. Q. Doe, 2014 Transient nuclear Prospero induces neural progenitor quiescence. eLife 3**:**
920 e03363.
921 Lanet, E., A. P. Gould and C. Maurange, 2013 Protection of neuronal diversity at the expense of neuronal
922 numbers during nutrient restriction in the Drosophila visual system. Cell reports 3**:** 587-594.
923 Larochelle, S., J. Pandur, R. P. Fisher, H. K. Salz and B. Suter, 1998 Cdk7 is essential for mitosis and for
924 in vivo Cdk-activating kinase activity. Genes & development 12**:** 370-381.
925 Larschan, E., M. M. Soruco, O. K. Lee, S. Peng, E. Bishop *et al.*, 2012 Identification of chromatin-
926 associated regulators of MSL complex targeting in Drosophila dosage compensation. PLoS Genet
927 8**:** e1002830.

928 Lee, C.-Y., R. O. Andersen, C. Cabernard, L. Manning, K. D. Tran *et al.*, 2006 Drosophila Aurora-A kinase
929 inhibits neuroblast self-renewal by regulating aPKC/Numb cortical polarity and spindle orientation.
930 Genes & development 20**:** 3464-3474.
931 Li, X., T. Erclik, C. Bertet, Z. Chen, R. Voutev *et al.*, 2013 Temporal patterning of Drosophila medulla
932 neuroblasts controls neural fates. Nature 498**:** 456-462.
933 Lin, D. M., and C. S. Goodman, 1994 Ectopic and increased expression of Fasciclin II alters motoneuron
934 growth cone guidance. Neuron 13**:** 507-523.
935 Love, M., S. Anders and W. Huber, 2014 Differential analysis of count data–the DESeq2 package. Genome
936 Biol 15**:** 10.1186.
937 Maroni, G., and S. Stamey, 1983 Use of blue food to select synchronous, late third instar larvae. Dros. Inf.
938 Serv 59**:** 142-143.
939 Morante, J., D. M. Vallejo, C. Desplan and M. Dominguez, 2013 Conserved miR-8/miR-200 defines a glial
940 niche that controls neuroepithelial expansion and neuroblast transition. Developmental cell 27**:**
941 174-187.
942 Neumüller, Ralph A., C. Richter, A. Fischer, M. Novatchkova, Klaus G. Neumüller *et al.*, 2011 Genome-
943 Wide Analysis of Self-Renewal in Drosophila Neural Stem Cells by Transgenic RNAi. Cell Stem
944 Cell 8**:** 580-593.
945 Pereanu, W., D. Shy and V. Hartenstein, 2005 Morphogenesis and proliferation of the larval brain glia in
946 Drosophila. Developmental biology 283**:** 191-203.
947 Prokop, A., and G. M. Technau, 1991 The origin of postembryonic neuroblasts in the ventral nerve cord of
948 Drosophila melanogaster. Development 111**:** 79-88.
949 Ramon-Cañellas, P., H. P. Peterson and J. Morante, 2018 From early to late neurogenesis: Neural
950 progenitors and the glial niche from a fly's point of view. Neuroscience.
951 Ramon-Cañellas, P., H. P. Peterson and J. Morante, 2019 From early to late neurogenesis: Neural
952 progenitors and the glial niche from a fly's point of view. Neuroscience 399**:** 39-52.

953 Raudvere, U., L. Kolberg, I. Kuzmin, T. Arak, P. Adler *et al.*, 2019 g:Profiler: a web server for functional
954 enrichment analysis and conversions of gene lists (2019 update). Nucleic Acids Research 47**:**
955 W191-W198.
956 Ribeiro, A. L., R. D. Silva, H. Foyn, M. N. Tiago, O. S. Rathore *et al.*, 2016 Naa50/San-dependent N-
957 terminal acetylation of Scc1 is potentially important for sister chromatid cohesion. Scientific
958 reports 6**:** 1-16.
959 Rieder, L. E., W. T. Jordan and E. N. Larschan, 2019 Targeting of the Dosage-Compensated Male X-
960 Chromosome during Early Drosophila Development. Cell Reports 29**:** 4268-4275.e4262.
961 Rieder, L. E., K. P. Koreski, K. A. Boltz, G. Kuzu, J. A. Urban *et al.*, 2017 Histone locus regulation by the
962 Drosophila dosage compensation adaptor protein CLAMP. Genes & development 31**:** 1494-1508.
963 Robinow, S., and K. White, 1988 The locus elav of Drosophila melanogaster is expressed in neurons at all
964 developmental stages. Developmental biology 126**:** 294-303.
965 Robinson, J. T., H. Thorvaldsdóttir, W. Winckler, M. Guttman, E. S. Lander *et al.*, 2011 Integrative
966 genomics viewer. Nature Biotechnology 29**:** 24-26.
967 Scadden, D. T., 2006 The stem-cell niche as an entity of action. Nature 441**:** 1075-1079.
968 Schmid, A., A. Chiba and C. Q. Doe, 1999 Clonal analysis of Drosophila embryonic neuroblasts: neural
969 cell types, axon projections and muscle targets. Development 126**:** 4653-4689.
970 Song, H.-J., J.-C. Billeter, E. Reynaud, T. Carlo, E. P. Spana *et al.*, 2002 The fruitless gene is required for
971 the proper formation of axonal tracts in the embryonic central nervous system of Drosophila.
972 Genetics 162**:** 1703-1724.
973 Soruco, M. M., J. Chery, E. P. Bishop, T. Siggers, M. Y. Tolstorukov *et al.*, 2013a The CLAMP protein
974 links the MSL complex to the X chromosome during Drosophila dosage compensation. Genes &
975 development 27**:** 1551-1556.
976 Soruco, M. M., J. Chery, E. P. Bishop, T. Siggers, M. Y. Tolstorukov *et al.*, 2013b The CLAMP protein
977 links the MSL complex to the X chromosome during Drosophila dosage compensation. Genes Dev
978 27**:** 1551-1556.

979 Sousa-Nunes, R., L. L. Yee and A. P. Gould, 2011 Fat cells reactivate quiescent neuroblasts via TOR and
980 glial insulin relays in Drosophila. Nature 471**:** 508-512.
981 Southall, T. D., C. M. Davidson, C. Miller, A. Carr and A. H. Brand, 2014 Dedifferentiation of neurons
982 precedes tumor formation in Lola mutants. Developmental cell 28**:** 685-696.
983 Speder, P., and A. H. Brand, 2018 Systemic and local cues drive neural stem cell niche remodelling during
984 neurogenesis in Drosophila. Elife 7**:** e30413.
985 Spéder, P., and A. H. Brand, 2014 Gap junction proteins in the blood-brain barrier control nutrient-
986 dependent reactivation of Drosophila neural stem cells. Developmental Cell 30**:** 309-321.
987 Tastan, Ö. Y., and J.-L. Liu, 2015 CTP synthase is required for optic lobe homeostasis in Drosophila.
988 Journal of genetics and genomics 42**:** 261-274.
989 Thurmond, J., J. L. Goodman, V. B. Strelets, H. Attrill, L. S. Gramates *et al.*, 2019 FlyBase 2.0: the next
990 generation. Nucleic acids research 47**:** D759-D765.
991 Tikhonova, E., A. Fedotova, A. Bonchuk, V. Mogila, E. N. Larschan *et al.*, 2019 The simultaneous
992 interaction of MSL2 with CLAMP and DNA provides redundancy in the initiation of dosage
993 compensation in Drosophila males. Development 146**:** dev179663.
994 Turki-Judeh, W., and A. J. Courey, 2012 Groucho: a corepressor with instructive roles in development, pp.
995 65-96 in *Current topics in developmental biology*. Elsevier.
996 Turner, F. R., and A. P. Mahowald, 1977 Scanning electron microscopy of Drosophila melanogaster
997 embryogenesis: II. Gastrulation and segmentation. Developmental biology 57**:** 403-416.
998 Udolph, G., P. Rath and W. Chia, 2001 A requirement for Notch in the genesis of a subset of glial cells in
999 the Drosophila embryonic central nervous system which arise through asymmetric divisions.
1000 Development 128**:** 1457-1466.
1001 Urban, J., G. Kuzu, S. Bowman, B. Scruggs, T. Henriques *et al.*, 2017 Enhanced chromatin accessibility of
1002 the dosage compensated Drosophila male X-chromosome requires the CLAMP zinc finger protein.
1003 PloS one 12**:** e0186855.

1004 Urban, J. A., Doherty, C. A, Jordan, W. T, Bliss, J. E, Feng, J., Soruco, M. M, Rieder, L. E, Tsiarli, M. A,
1005 Larschan, E. N, 2017 The essential Drosophila CLAMP protein differentially regulates non-coding
1006 roX RNAs in male and females. Chromosome Research 25**:** 101-113.
1007 Weake, V. M., K. K. Lee, S. Guelman, C. H. Lin, C. Seidel *et al.*, 2008 SAGA-mediated H2B
1008 deubiquitination controls the development of neuronal connectivity in the Drosophila visual
1009 system. The EMBO journal 27**:** 394-405.
1010 Wei, J.-Y., P.-C. Chung, S.-Y. Chu and H. H. Yu, 2019 FOXO regulates cell fate specification of
1011 Drosophila ventral olfactory projection neurons. Journal of neurogenetics 33**:** 33-40.
1012 Xiong, W.-C., H. Okano, N. H. Patel, J. A. Blendy and C. Montell, 1994a repo encodes a glial-specific
1013 homeo domain protein required in the Drosophila nervous system. Genes & development 8**:** 981-
1014 994.
1015 Xiong, W. C., H. Okano, N. H. Patel, J. A. Blendy and C. Montell, 1994b repo encodes a glial-specific
1016 homeo domain protein required in the Drosophila nervous system. Genes & Development 8**:** 981-
1017 994.
1018 Yildirim, K., J. Petri, R. Kottmeier and C. Klämbt, 2019 Drosophila glia: Few cell types and many
1019 conserved functions. Glia 67**:** 5-26.
1020 Yu, G., L.-G. Wang, Y. Han and Q.-Y. He, 2012 clusterProfiler: an R package for comparing biological
1021 themes among gene clusters. Omics: a journal of integrative biology 16**:** 284-287.
1022 Yuan, X., C. W. Sipe, M. Suzawa, M. L. Bland and S. E. Siegrist, 2020 Dilp-2–mediated PI3-kinase
1023 activation coordinates reactivation of quiescent neuroblasts with growth of their glial stem cell
1024 niche. Plos Biology 18**:** e3000721.
1025 Yuasa, Y., M. Okabe, S. Yoshikawa, K. Tabuchi, W. C. Xiong *et al.*, 2003 Drosophila homeodomain
1026 protein REPO controls glial differentiation by cooperating with ETS and BTB transcription factors.
1027 Development 130**:** 2419-2428.

1028 Zaharieva, E., I. U. Haussmann, U. Brauer and M. Soller, 2015 Concentration and Localization of
1029 Coexpressed ELAV/Hu Proteins Control Specificity of mRNA Processing. Mol Cell Biol 35: 3104-
1030 3115.
1031

1032 **Acknowledgements**

1033 We thank Dr. Edward A. Kravitz for providing MAT laboratory space and contributing to supply costs for
1034 completion of this study, Dr. Yick-Bun Chan for experimental support and assistance with DEG analysis
1035 and Dr. Yiannis Savva for experimental support. We would also like to thank Dr. Séverine Trannoy for
1036 critical reading of this manuscript. We thank the Harvard Medical School Neurobiology Department and
1037 the Neurobiology Imaging Facility for consultation and instrument availability that supported this work.
1038 This facility is supported in part by the Neural Imaging Center as part of an NINDS P30 Core Center grant
1039 #NS072030. This work was supported in part by a Harvard Medical School Fix Fund Postdoctoral
1040 Fellowship to M.A.T and by US National Institute of Health grants to E.N.L and E.A.K (R35 GM126994-
1041 01 and R35 GM118137).
1042

1043 **Contributions**

1044 MAT and E.N.L conceived the study and M.A.T designed the study. M.A.T performed
1045 immunohistochemistry and imaging, collection of RNA-seq samples and analysis of RNA-seq DEG results.
1046 L.X contributed to sample collection for RNA-seq experiments and immunohistochemistry, E.N
1047 contributed in size experiments, A.M.C contributed in RNA-seq data analysis and JK in ChIP-seq data
1048 analysis. M.A.T prepared figures and wrote the original draft while M.A.T and E.N.L curated the
1049 manuscript with input from all authors.
1050

1051 **Declaration of Interests**

1052 The authors declare no competing interests.
1053

1054

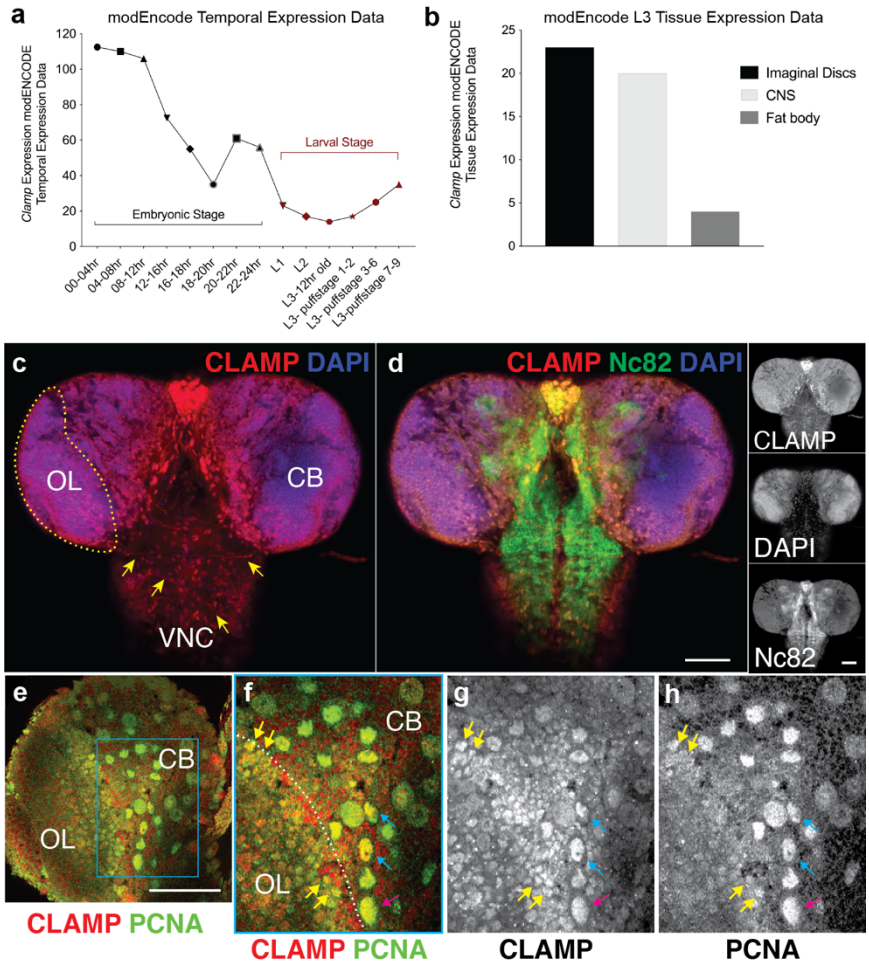

1055

1056 **Figure 1 CLAMP is ubiquitously expressed throughout the L3 nervous system and is present in**
1057 **proliferating neuroblasts.** (a) Temporal expression data from modEncode (Flybase) reveal that *clamp*
1058 expression levels decrease as embryonic development proceeds and as the maternal transcripts are used-up
1059 and reach a nadir at 18-20 hours after egg lay, which is then followed by a sharp increase just before
1060 embryonic development is completed. During the larval stages *clamp* expression decreases until L3, where
1061 it slowly starts to increase again before the pupa stage. (b) Tissue specific L3 expression data, reveal that
1062 *clamp* is most highly expressed in the developing imaginal disks, the CNS and the fat body.
1063 (c-d) CLAMP is expressed both in the L3 central nervous system, specifically in the optic lobe (OL, yellow
1064 dashed outline), central brain, (CB) and in the ventral nerve cord (VNC). CLAMP is present in the nucleus
1065 throughout the nervous system as seen by co-staining with DAPI and Nc82, which marks the synaptic

1066 processes. In the VNC it is also observed in the neuronal processes (c, arrows). Grayscale panels show
1067 individual staining channels. (e-h) Higher resolution images reveal high expression of CLAMP in the
1068 developing CB and OL and in proliferating NSCs marked by Proliferating cell nuclear antigen (PCNA). (f-
1069 h) Magnification of the boxed area in panel e, reveals that CLAMP is present in CB cycling neuroblasts
1070 and mother ganglion cells (magenta and cyan arrows, respectively). Scale bars: 50 μm and 25 μm in j.
1071
1072
1073
1074
1075
1076
1077

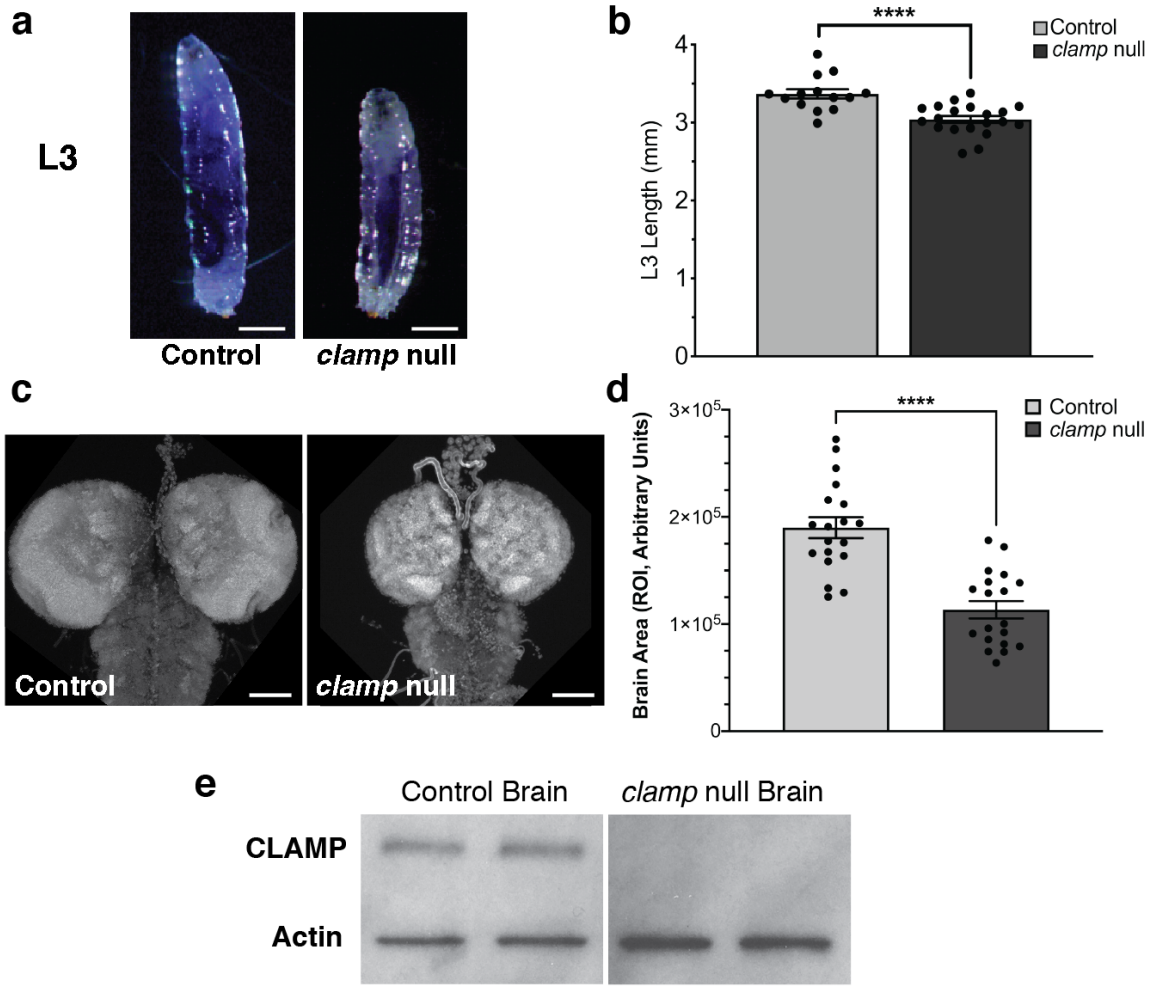

1078

1079

1080 **Figure 2 Lack of CLAMP results in growth deficits both in the body and the nervous system** (a, b)
1081 Mutant *clamp* null L3 larvae are considerably smaller in size, compared to control L3s (Mean length ±
1082 SEM; Control: 3.369 ± 0.06031, n=14; *clamp* null: 3.041 ± 0.04371, n=20; ttest p< 0.0001). (c, d) This
1083 reduction is maintained at the CNS level of *clamp* null L3 larvae (Mean normalized brain area ± SEM;
1084 Control: 1.001 ± 0.0485, n=20; *clamp* null: 0.601 ± 0.04052, n=20; ttest p< 0.0001). (e) Western blot for
1085 CLAMP in samples from L3 brain lysates from control and *clamp* null L3 showing the absence of CLAMP
1086 protein (n=2 per condition). Scale bars: 1 mm in a; 50 µm in c.

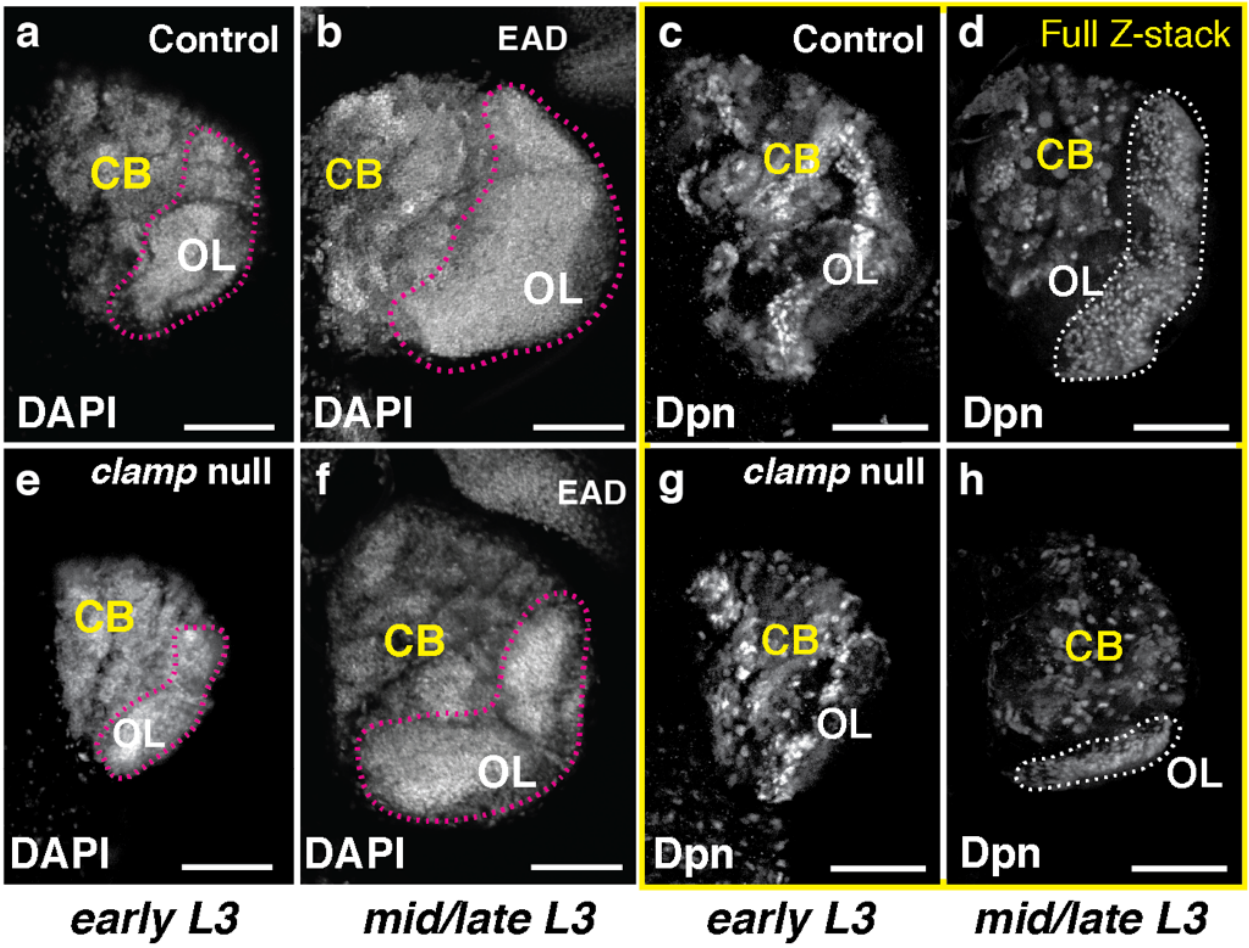

1087

1088 **Figure 3 Lack of CLAMP greatly affects brain development and causes defects in optic lobe**
1089 **formation.** (a, b and e, f) Brain development in the *clamp* null L3 is severely impaired from the early L3
1090 stage, while even at the mid/late L3 stage, *clamp* null brains resemble early L3 control brains. (c, d and g,h)
1091 Full z-stacks of L3 brains showing the distribution of Deadpan (Dpn) -positive NSCs areas, reveals that
1092 NSCs development both in the central brain (CB) and the optic lobe (OL) of the null are impaired, starting
1093 from the early L3 stage and continuing to the mid/late L3 stage. Especially impaired is the OL development
1094 as seen by the reduction in the Dpn+ area indicated with the white dashed outlined areas. EAD: eye antenna
1095 disk. Panels a, b, e and f are 3 optical sections whereas c, d, g and h are full z-stacks throughout the brain.
1096 Scale bars: 50 μm.

Developmental RNA-sequencing

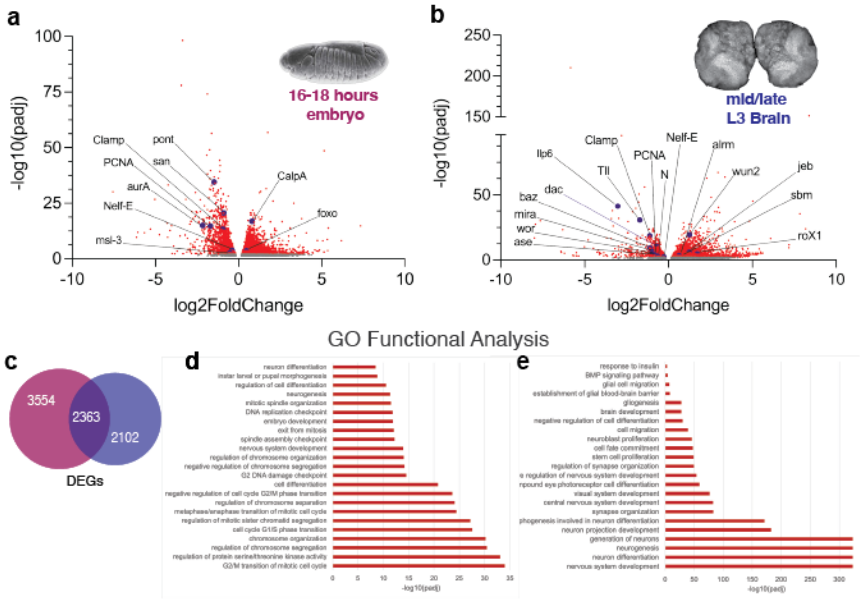

f CLAMP Binding Motif Analysis (FIMO)

Gene	Function
pont	NB attributes
aurA	NB self-renewal; spindle orientation
apc7	Chromosome segregation
esc	NB proliferation
fru	Axonal projections
san	Sister chromatin cohesion
baz	Asymmetric cell division
pcna	Cell cycle dynamics
notch	NB attributes; stem cell division
cdk7	Mitosis regulator
Nelf-E	Transcriptional pausing
sbm	Neural development regulation *via* ecdysone signaling
gcm	Master regulator of gliogenesis
tll	Optic lobe development
gbb	NB proliferation and surface glia survival
D	Regulation of neuronal fate in the OL
Alk	Cell cycle regulation and NB proliferation
wun	Regulates bioactive lipid levels

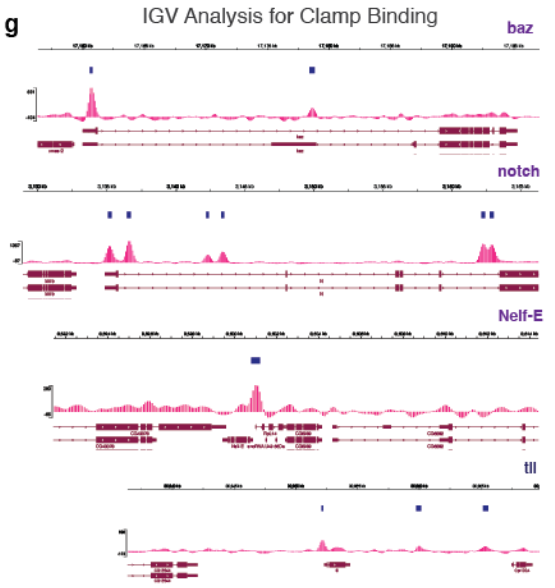

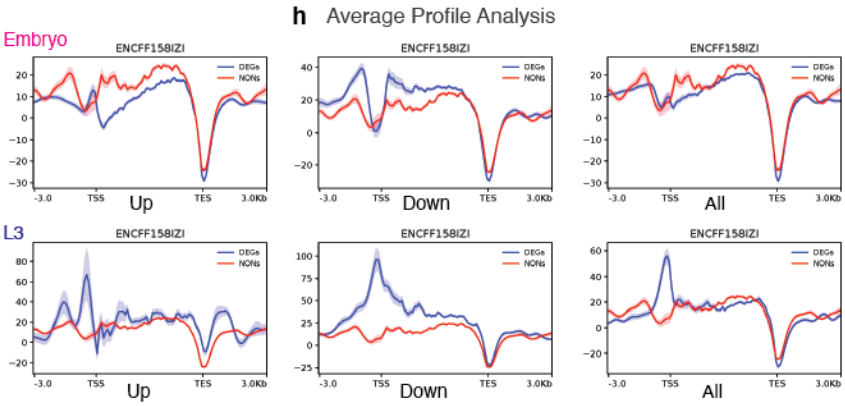

1097

1098 **Figure 4 CLAMP is implicated in transcriptomic networks that regulate the proliferation and**
1099 **differentiation of NSCs.** (a, b) Experimental workflow for RNA sequencing data generation and DEG
1100 meta-analysis. Embryo panel is scanning electron image of a late stage embryo from(TURNER AND
1101 MAHOWALD 1977). (c) Venn diagram of DEGs in the *clamp* null embryo and L3. (d,e) GO analysis of the
1102 *clamp* null DEGs revealed high enrichment in categories related to cell cycle dynamics and neural
1103 development. (f) Find Individual Motif Occurrences (FIMO) analysis of the DEGs for the CLAMP binding
1104 motif, revealed that critical regulators of neural development and mitosis are putative targets for CLAMP
1105 binding both at the embryonic and L3 stage, (g) while analysis of embryo ChIP-seq data revealed a direct
1106 regulation of *Tll, Notch, baz* and *Nelf-E* by CLAMP. (h) Average binding profiles for the upregulated
1107 and downregulated DEGs in embryo and L3 *clamp* null. Gene regions were scaled to match
1108 positions of the transcription start sites (TSS) and transcription end sites (TES) with 3k base pairs
1109 shown on either side of the gene. For comparison in each image, the average read depth is also
1110 plotted for 2571 gene regions that show expression in the nervous system but are not differentially
1111 expressed in any of these RNA-seq experiments (NONs). The shaded region around each line is
1112 the standard error of the mean. The genes downregulated in the absence of clamp show higher
1113 average read depth around the TSS, particularly in larvae.
1114
1115
1116
1117
1118
1119
1120
1121
1122
1123
1124
1125
1126

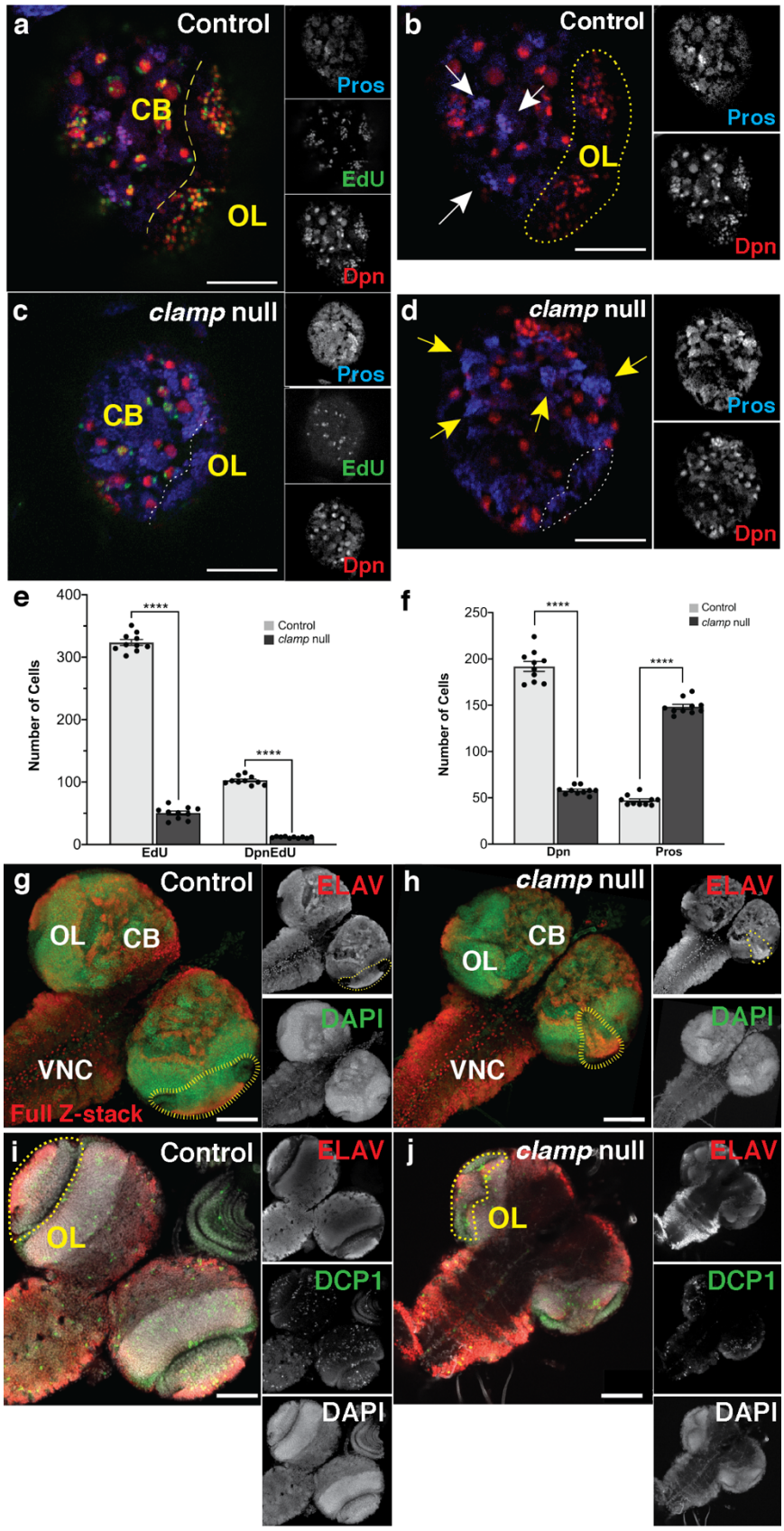
a
Control
CB
OL
Pros
EdU
Dpn
b
Control
OL
Pros
Dpn
c
clamp null
CB
OL
Pros
EdU
Dpn
d
clamp null
Pros
Dpn
e
Number of Cells
400
300
200
100
0
****
****
Control
clamp null
EdU
DpnEdU
f
Number of Cells
250
200
150
100
50
0
****
****
Control
clamp null
Dpn
Pros
g
Control
OL
CB
VNC
Full Z-stack
ELAV
DAPI
h
clamp null
OL
CB
VNC
ELAV
DAPI
i
Control
OL
ELAV
DCP1
DAPI
j
clamp null
OL
ELAV
DCP1
DAPI

1127

1128 **Figure 5 Lack of CLAMP impairs neural stem cell proliferation and promotes precocious**
1129 **differentiation**. (a-d) Proliferation of NSCs as seen by EdU labeling, is highly reduced in the *clamp* null
1130 brain, with the most evident impact being on OL NSCs (panels a and c, dashed lines indicate the OL). In
1131 parallel, nuclear Pros+ clusters indicate acquisition of neuronal fate, are more evident in the *clamp* null
1132 brains (panels b and d, arrows). (e) Both the total number of proliferating stem cells (EdU^+ Mean ± SEM,
1133 Control: 323.6 ± 4.679; *clamp* null: 50.40 ± 3.174; $p<0.0001$; n=10) and of proliferating Dpn^+ NSCs is
1134 reduced (Dpn^+EdU^+ Mean ± SEM; Control 102.6 ± 2.141; *clamp* null 11.50 ± 0.3727; n=10). (f) The
1135 reduction in total Dpn+ cells (Dpn^+ Mean ± SEM, Control: 191.9 ± 5.313; *clamp* null: 57.90 ± 1.402; p
1136 <0.0001; n = 10), is accompanied by a respective increase in Pros+ cells in the *clamp* null brains ($Pros^+$
1137 Mean ± SEM, Control: 47.1 ± 1.716; *clamp* null: 148.3 ± 2.629; $p <0.0001$; n = 10). (g, h) Additionally,
1138 despite having an increase in the neuronal marker Elav in the *clamp* null brains, the OL development is
1139 impaired compared to controls (outlines). (i, j) Apoptotic cells marked with DCP1 are more in the OL of
1140 the null compared to a more ubiquitous distribution in the control. CB, central brain; OL, optic lobe; VNC:
1141 ventral nerve cord. Scale bars: a-d, 100 µm; g and h, 50 µm.
1142
1143

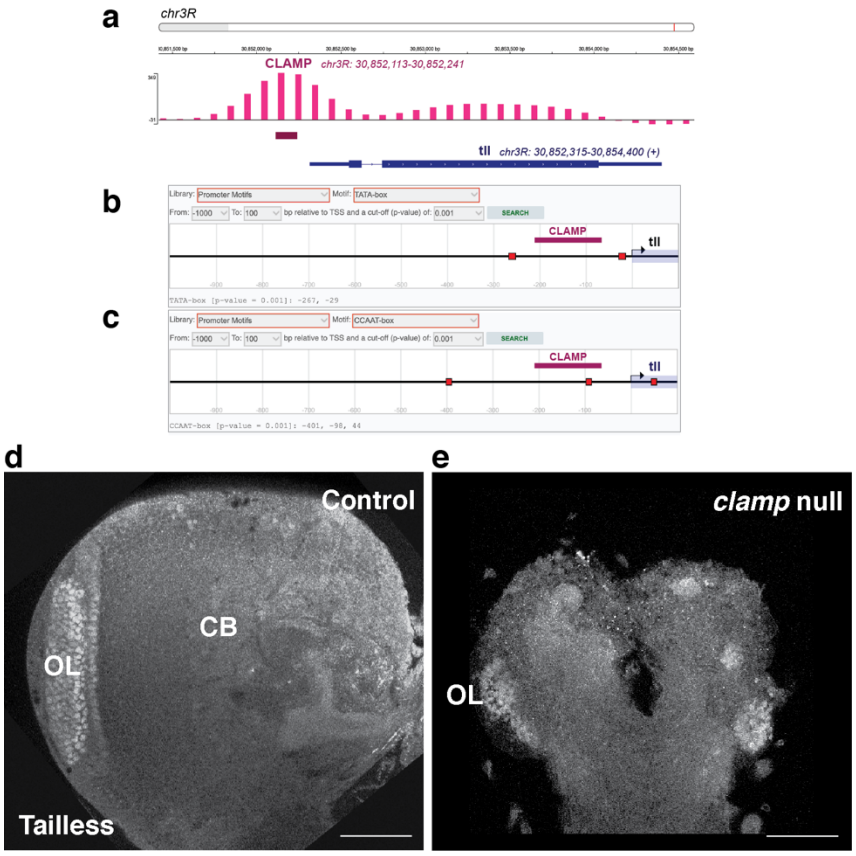

Figure 6 Direct regulation of *Tailless* by CLAMP causes an almost complete absence of its expression in the OL. (a-c) Analysis of embryo ChIP-seq data reveal that CLAMP directly binds to the *Tailless* gene in putative promoter areas. (d,e). Expression of the Tailless protein is almost absent in the clamp null optic (OL) lobe which is severely underdeveloped. Central brain (CB). Scale bars, 50 µm.

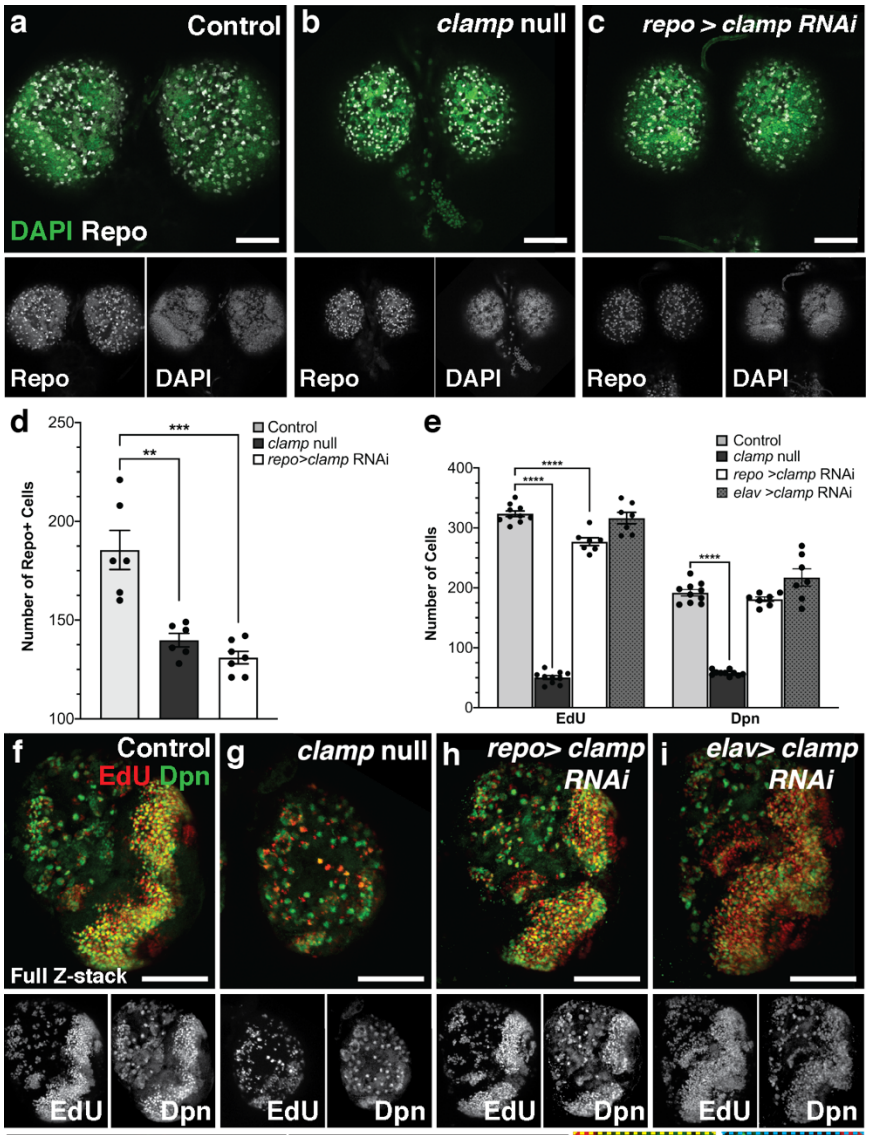

Figure 7 Glial-CLAMP surface glia generation and NSC proliferation (a-e) Surface glia (SG) is reduced by ~25% in the *clamp* null brain compared to controls (% SG Repo$^+$ ± SEM, *Control*: 99.98 ± 5.328; *clamp* null: 75.37 ± 1.843; n=6) whereas, (e-i) proliferating NSCs (EdU$^+$ ± SEM, *Control:* 323.6 ± *4.679; clamp* null: 50.40 ± *3.174*) and NSCs (Dpn$^+$ ± SEM, *Control:* 191.9 ± *5.313; clamp* null: 57.90 ± *1.402*) are also reduced in numbers. Glial-specific *clamp* knock-down (*repo>clamp RNAi*) promotes a similar reduction in SG numbers ((% SG Repo$^+$ ± SEM, *repo>clamp RNAi* 131.0 ± 3.162) and promotes a reduction in proliferating NSCs (*repo>clamp RNAi* EdU$^+$ ± SEM*:* 277 ± 6.572; Dpn$^+$ ± SEM: 181 ± 3.964), but to a lesser extend as the one seen in the *clamp* null. Neuronal-specific clamp KD (*elav>clamp RNAi*)

1170 does not affect NSC proliferation and numbers NSCs (*elav>clamp RNAi* EdU^+ ± SEM*:* 316. ± 9.519; Dpn^+

1171 ± SEM: 217 ± 14.45). Scale bars 100 µm.

1172

1173

1174

Gene Name	log2FC	padj
elav	0.44	0.043
ewg	NA	NA
clamp	-1	6.39E-14
CG12299	-0.70	0.0001
gro	-0.88	2.45E-06
CG8924	-1.12	1.15E-10
JIL-1	NA	NA
osk	-4.76	1.67E-11
ac3	0.54	4.87E-05
cdc16	-0.83	0.005
Ibf1	-0.78	0.0002
Bcl7-like	-0.93	2.92E-11

1175

1176

1177

1178

1179

1180

1181

1182

1183

1184

1185

1186

1187

1188

1189 *Table 1: Functional interactors of clamp as identified by Haussman et al., 2008*

1190

1191

1192

1193

1194

1195

Gene ID	***Gene Name***	***Log2FC***	***padj***	***Function***
FBgn0044047	*Dilp6*	-3.028	4.38E-42	OL development/Glia Neuroblast interactions/Insulin Signaling
FBgn0003720	*tll*	-1.71	1.89E-31	OL development
FBgn0031745	*rau*	-1.373	3.42E-18	Glial cell development/differentiation of neurons and glia in the developing eye.
FBgn0014179	*gcm*	-1.281	5.90E-12	Glial cell development-promotes gliogenesis over neurogenesis
FBgn0010433	*ato*	-1.246	3.88E-15	OL development
FBgn0000529	*bsh*	-1.155	1.85E-24	OL development
FBgn0019809	*gcm2*	-1.154	3.97E-20	Has a redundant role with the product of *gcm* in the differentiation of glial cells and subset of neurons(CHOTARD *et al.* 2005).
FBgn0031375	*erm*	-1.116	2.76E-19	Cell fate regulator during neurogenesis.
FBgn0000163	*baz*	-1.105	6.44E-10	Bazooka forms a complex with par-6 and aPKC. Functions in cell polarization and ACD.
FBgn0021776	*mira*	-0.99	3.16E-07	Neuroblast proliferation.
FBgn0000137	*ase*	-0.972	1.54E-05	Type I NB attributes.
FBgn0263512	*Vsx2*	-0.956	9.10E-23	OL development.
FBgn0010382	*CycE*	-0.951	0.00131	Cell cycle dynamics.
FBgn0001983	*wor*	-0.94	3.01E-05	Worniu, neuroblast attributes.
FBgn0000320	*eya*	-0.909	2.05E-08	OL development /insulin producing cells differentiation.
FBgn0000404	*CycA*	-0.855	0.010084	Cell cycle progression including G2.
FBgn0025739	*pon*	-0.847	3.66E-07	Contributes to asymmetric localization of numb and the subsequent suppression of Notch signaling.
FBgn0002973	*numb*	-0.845	1.67E-15	Acts via Notch signaling, asymmetric division control.
FBgn0005655	*PCNA*	-0.824	0.00019	Cell cycle dynamics.
FBgn0011674	*insc*	-0.788	1.44E-06	Spindle orientation; asymmetric divisions.
FBgn0037913	*fabp*	-0.72	1.85E-06	Expressed in lipid droplet-forming glial cells.
FBgn0013469	*klu*	-0.713	0.00013	Klumpfuss (*klu*) is a temporal fate determination.
FBgn0005677	*dac*	-0.707	4.97E-11	OL development.
FBgn0010109	*dpn*	-0.665	0.00245	Neuroblast self-renewal -interacts with *klu* and *erm*.
FBgn0004647	*Notch*	-0.642	0.0018	OL development/Stem cell proliferation.
FBgn0000411	*Dichaete (D)*	-0.634	2.56E-08	Nervous system development and OL development.
FBgn0044324	*Chro*	-0.61	0.00021	Neuroblast proliferation. Functions downstream of InR/PI3K/TOR signaling and regulates expression of quiescence-inducing Pros to permit NSC reactivation.
FBgn0005427	*ewg*	-0.533	1.06E-06	Neurogenesis/Synaptogenesis.
FBgn0040080	*pins*	-0.52	0.008985	Partner of Inscutable; involved in ACD and establishment of cell polarity.

1196 *Table 2: Down-regulated genes in the clamp null L3 brain*

Gene ID	***Gene Name***	***Log2Fc***	***padj***	***Function***
FBgn0000014	abd-A	2.983	0.00019	Controls the end of neuroblast proliferation.
FBgn0025879	Timp	2.299	9.57E-23	Coordinates synaptogenesis
FBgn0001258	Ldh	2.353	2.43E-22	Lipid metabolism.
FBgn0003117	pnr	2.106	0.008812	Activator of *proneural* achaete-scute complex genes.
FBgn0011746	ana	1.831	3.97E-20	Encodes a secreted glycoprotein that is expressed in glia and at lower levels in neuroblasts, suppresses neuroblast proliferation.
FBgn0032006	Pvr	1.742	8.56E-22	Glia development /neuroblast proliferation.
FBgn0016032	lbm	1.576	3.84E-21	facilitates synapse assembly
FBgn0037989	ATP8B	1.664	2.18E-20	Flippase, translocates phospholipids from one side of a membrane to the other forming new membrane structures, especially vesicles.
FBgn0031461	daw	1.502	2.82E-05	Regulates insulin release from IPC neurons.
FBgn0041087	wun2	1.249	3.17E-20	Encodes a lipid phosphate phosphatase; expressed in astrocytes.
FBgn0086677	jeb	1.224	1.37E-06	Functions as signaling ligand for the product of Alk.
FBgn0066101	LpR1	0.899	3.91E-21	Cellular uptake of neutral lipids from the circulating protein encoded by apolpp.
FBgn0000416	Sap-r	0.889	2.23E-29	Lysosomal Lipid homeostasis.
FBgn0000546	EcR	0.847	6.72E-06	Ecdysone Receptor.
FBgn0040505	Alk	0.692	0.00014	Employs Ras/ERK and PI3K signalling pathways, functions in multiple contexts including synaptic signaling.
FBgn0001297	kay	0.699	7.62E-12	Specifically expressed in glia.
FBgn0039332	alrm	0.635	0.00038	Glial related.
FBgn0000370	crc	0.61	3.83E-17	Coactivator of the product EcR, promotes expression the molting peptide hormone encoded by ETH.
FBgn0016078	wun	0.558	2.85E-07	Lipid phosphate phosphatase.
FBgn0013342	nSyb	0.506	3.24E-05	Synaptic signaling.
FBgn0030574	sbm	0.504	0.002373	L-type amino acid transporter expressed in glia; essential for proper timing of development and brain growth (GALAGOVSKY *et al.* 2018).

1197 *Table 3: UP-regulated genes in the clamp null L3 brain*

1198

1199

1200

1201

1202

1203

1204

1205

Supplementary figures

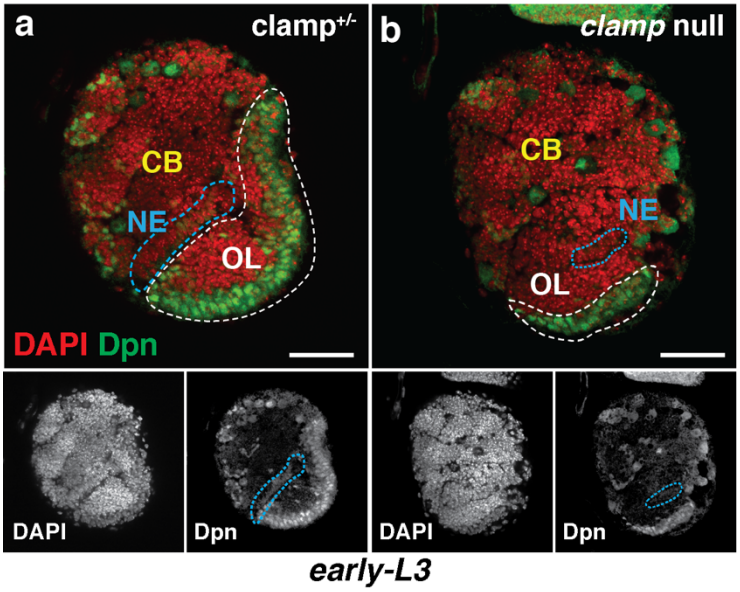

Supplementary Figure 1: A single dose of the *Clamp* gene is sufficient to allow for normal brain development. NE, neuroepithelium; OL, optic lobe; CB, central brain. Scale bars 100 µm

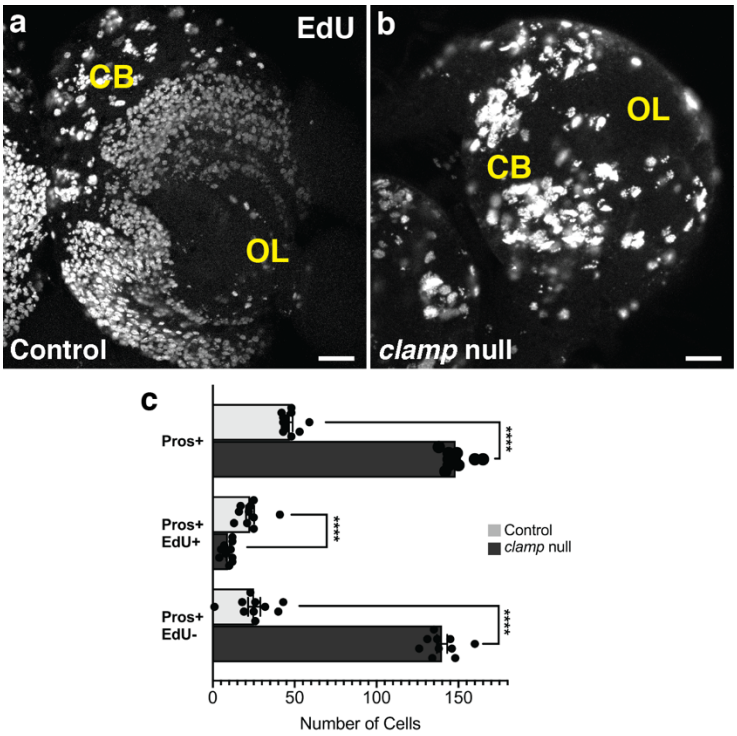

1224

1225 **Supplementary Figure 2: Proliferation on neural stem cells is impaired in the absence of CLAMP.**

1226 OL, optic lobe; CB, central brain. Scale bars 100 µm

1227

1228

1229

1230

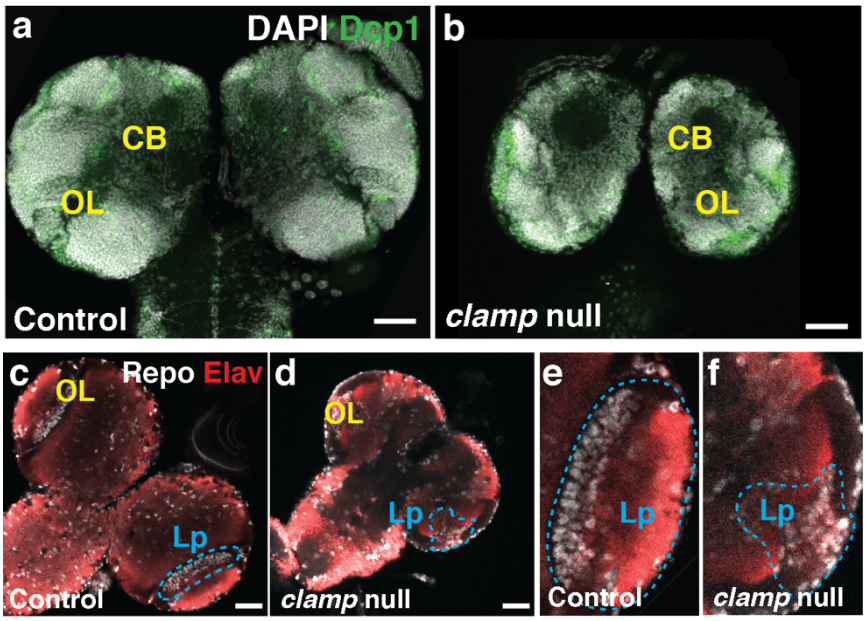

Supplementary figure 3: Absence of CLAMP results in increased cell death, especially in the optic lobe's Lobula plug. Lp**,** Lobula plug; OL, optic lobe; CB, central brain. Scale bars 100 µm